



The Continuous Electron Beam Accelerator Facility  
Theory Group Preprint Series

WM-95-101  
CEBAF-TH-95-04

Additional copies are available from the authors.

The Southeastern Universities Research Association (SURA) operates the Continuous Electron Beam Accelerator Facility for the United States Department of Energy under contract DE-AC05-84ER40150

Unitary, gauge invariant, relativistic resonance model  
for pion photoproduction

Yohanes Surya  
*College of William and Mary, Williamsburg, VA 23185, USA*

Franz Gross  
*College of William and Mary, Williamsburg, VA 23185, USA*  
and  
*Continuous Electron Beam Accelerator Facility*  
*12000 Jefferson Ave, Newport News, Virginia 23606, USA*

DISCLAIMER

This report was prepared as an account of work sponsored by the United States government. Neither the United States nor the United States Department of Energy, nor any of their employees, makes any warranty, express or implied, or assumes any legal liability or responsibility for the accuracy, completeness, or usefulness of any information, apparatus, product, or process disclosed, or represents that its use would not infringe privately owned rights. Reference herein to any specific commercial product, process, or service by trade name, mark, manufacturer, or otherwise, does not necessarily constitute or imply its endorsement, recommendation, or favoring by the United States government or any agency thereof. The views and opinions of authors expressed herein do not necessarily state or reflect those of the United States government or any agency thereof.

# Unitary, gauge invariant, relativistic resonance model for pion photoproduction

Yohanes Surya

*College of William and Mary, Williamsburg, VA 23185, USA*

Franz Gross

*College of William and Mary, Williamsburg, VA 23185, USA*

and

*Continuous Electron Beam Accelerator Facility*

*12000 Jefferson Ave, Newport News, Virginia 23606, USA*

## Abstract

Pion photoproduction up to 770 MeV photon laboratory energy is described by a manifestly covariant wave equation, which includes a treatment of the final state  $\pi N$  interactions consistent with the covariant, unitary, resonance model of  $\pi N$  scattering previously developed. The kernel of the equation includes nucleon ( $N$ ), Roper ( $N^*$ ), Delta ( $\Delta$ ), and  $D_{13}$  poles and their crossed poles, as well as  $\pi$ ,  $\rho$ , and  $\omega$  exchange terms. The Kroll-Rudermann term and other interaction currents insure that the model is exactly gauge invariant to all orders in the strong coupling,  $g_{\pi NN}$ , and that the low energy theorem is satisfied. Unitarity is maintained up to first order in the charge  $e$  (Watson theorem). The complete development of this model, which gives a good fit to all the data up to 770 MeV, is presented.

## I. OVERVIEW, RESULTS AND CONCLUSIONS

### A. Introduction

Pion photoproduction has been studied for many years. One of the earliest models, developed by Chew, Goldberger, Low and Nambu, is based on dispersion theory [1]. It included nucleon Born terms and  $\Delta$ -excitation and described the reaction up to 500 MeV photon lab energy. Further study (using pseudoscalar  $\pi NN$  coupling) was undertaken by Donnachie [2]. Among later efforts is the work based on chiral lagrangians carried out by Olsson and Osypowski [3]. They used pseudovector  $\pi NN$  coupling and also introduced  $\omega$  exchange. This work was further developed by Wittman, et al. [4]. More recently, Nozawa, Blankleider and Lee [5] developed a dynamical model of pion photoproduction in which they used a separable interaction to describe the final state  $\pi N$  interactions. Lee and Pearce [6] improved on this description by using a reduction of Bethe-Salpeter equation to treat the meson nucleon interaction in the final state. They calculated photoproduction observables up to 500 lab photon energy. However, with the construction of powerful new facilities such as the Continuous Electron Beam Accelerator Facility (CEBAF), it is necessary to have a good description of pion photoproduction which extends up to higher energies. Such description must be covariant, gauge invariant to all order of the strong coupling constants, and include not only the nucleon ( $N$ ) and delta ( $\Delta$ ) resonances, but also the Roper ( $N^*$ ) which plays a prominent role in the isospin  $\frac{1}{2}$  amplitudes and the  $D_{13}$  (1520) which makes large contributions to  $D$ -waves.

In this paper we present a simple, covariant, gauge invariant and unitary

model for  $\pi$  photoproduction which works well up to 770 MeV photon lab energy. This model is fully consistent with a slightly modified version of our previously published model for  $\pi N$  scattering [7], described in Sec. III. The modifications in the  $\pi N$  model were made in order to (i) improve the threshold behaviour (scattering lengths), (ii) more faithfully approximate the physics of the  $\pi\pi N$  channels which account for the inelasticity, (iii) have a better form factor for further extensions of the model and (iv) reduce the complexity of the  $\pi\gamma$  interaction currents by minimizing the energy dependence of the  $\pi N$  interaction kernel which generates these interaction currents. We have introduced a new form for the  $\pi N\Delta$  and  $\pi ND_{13}$  vertices which makes the calculations simpler. At all times we have tried to keep both the  $\pi N$  and  $\pi$  photoproduction models as simple as possible (without sacrificing essential physics) so that they may be *consistently* used as input to  $NN$  scattering and deuteron photodisintegration calculations.

In this work the pion photoproduction multipole amplitudes are obtained from the solution of a relativistic wave equation, in which the pion is restricted to its mass shell in all intermediate states except in the pion pole diagram, which is needed to keep gauge invariance. The rationale for this approach is described in our  $\pi N$  paper [7]. As in  $\pi N$  scattering, in order to describe the resonances at photon lab energy  $\sim 300$ ,  $\sim 450$ , and  $\sim 760$  MeV, the kernel or driving terms of the relativistic integral equation include undressed  $\Delta$ ,  $N^*$ , and  $D_{13}$  poles in addition to the undressed nucleon pole. The kernel also includes contributions derived from crossed  $N$ ,  $\Delta$ ,  $N^*$ , and  $D_{13}$  diagrams and from  $\omega$  and  $\rho$  exchange terms. The  $\omega$  exchange is claimed to give a significant contribution to the  $M_{1+}(\frac{1}{2})$  amplitude and  $M_{1-}(\frac{1}{2})$  amplitudes (for an explanation of the multipole notation see subsection B below, and Appendix B) [3]. Although the  $\rho$  exchange contribution is claimed to be small [8], it is still included in our model. We believe that it will contribute to the  $M_{1-}(1/2)$  and  $M_{2-}(1/2)$  channels. Besides that we also would like to get an estimate of the strength of the  $\rho\pi\gamma$  interaction. Our approximation scheme makes the crossed  $\Delta$  and  $D_{13}$  poles zero, as in the  $\pi N$  model. This makes the model simpler and the numerical calculations easier, and is consistent with other approximations we have made. The crossed nucleon pole is treated exactly because of its importance in the proof of gauge invariance, and the crossed Roper is also treated exactly because it has the same properties as the nucleon. All of these driving terms are shown diagrammatically in Fig. 1. The Kroll-Ruderman term (contact diagram) and the additional interaction currents needed to make the model gauge invariant are described in Secs. II and IV. The solution which emerges from the integral equation (which includes the Born terms shown in Fig. 1 plus the final state interactions illustrated in Fig. 2), automatically satisfies unitarity up to the first order in  $e$  (referred to as the Watson theorem) [9].

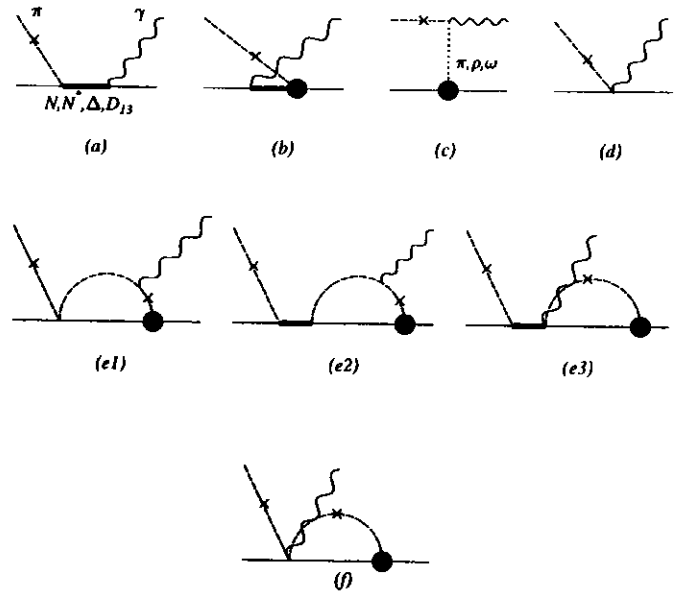


Figure 1: Diagrammatic representation of the driving terms for pion-photoproduction. Pions are dashed lines (with an  $\times$  if it is on shell), baryons are solid lines, and the big solid circles represent fully dressed vertex functions, as discussed in Sec. II.

Features of our  $\pi$  photoproduction model which are consistent with the  $\pi N$  scattering model include the following: (i) the  $\pi NN$  coupling is taken to be a superposition of both pseudoscalar ( $\gamma_5$ ) and pseudovector ( $\gamma^\mu\gamma_5$ ) coupling; (ii) the nucleon self energy is constrained to be zero at the nucleon pole, so that the nucleon mass remains unshifted by the interaction; (iii) contributions from the Roper ( $N^*$ ) and ( $N^* \leftrightarrow N$ ) transition amplitudes are iterated to all orders, giving a consistent description of the Roper and its width; and (iv) the  $\Delta$  and  $D_{13}$  are treated as pure spin 3/2 particles, which the same propagators used in the  $\pi N$  model.

In the remainder of this section we will describe the history and background

## B. The $E2/M1$ ratio

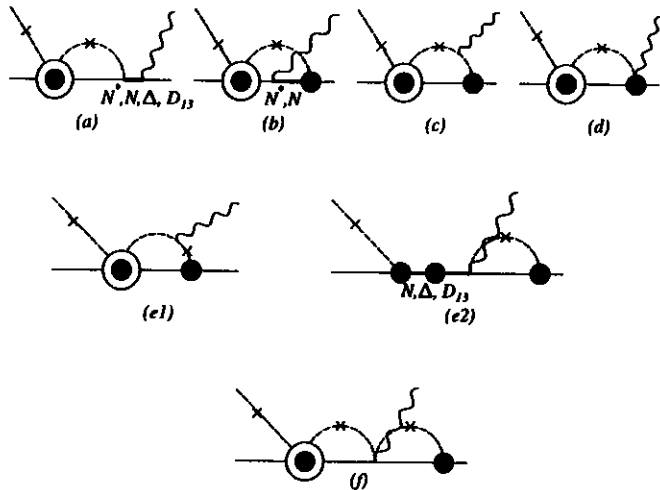


Figure 2: Diagrammatic representation of the final state interactions for pion-photoproduction. The solid circle surrounded by an open circle represents the full  $\pi N$  scattering amplitude.

of some aspects of pion photoproduction such as the  $E2/M1$  ratio, low energy theorem, unitarity, and gauge invariance. The general theory is described in Sec. II. After a description of the modifications in the  $\pi N$  model given in Sec. III, the  $\pi$  photoproduction model is described in Sec. IV. The Appendices discuss some technical points.

The tensor interaction between quarks, such as the one which arises from the one-gluon-exchange interaction, gives a small  $D$  state admixture to the predominantly  $S$  state wave functions of the nucleon and the  $\Delta$ . This tensor interaction leads to a resonant electric quadrupole amplitude  $E_{1+}(\frac{3}{2})$  (or  $E2$ ) which is very small compared to the resonant magnetic dipole amplitude  $M_{1+}(\frac{3}{2})$  (or  $M1$ ). [Here the amplitudes are denoted by  $E_{l\pm}(I)$  and  $M_{l\pm}(I)$ , where  $l$  is the orbital angular momentum of the photoproduced pion, the  $\pm$  sign refers to the total  $\pi N$  angular momentum  $j = l \pm 1/2$ , and  $I$  is the isospin of the  $\pi N$  system. The non vanishing  $E2$  amplitude is one of the signals of the  $D$  state admixture. Therefore it is important to determine the  $E2$  amplitude in order to test various quark model predictions.

There have been several attempts to measure the  $E2$  amplitude, but it is difficult to get an accurate value because the  $E2$  amplitude is very small compared to the dominant  $M1$  amplitude, and the background is comparatively large [10]. The analyses of the data using several models shows that although all of the calculations agree that  $E2$  is small, there is considerable uncertainty as to its precise size. Results for the  $E2/M1$  ratio which are listed in the Review of Particle Properties [11] are  $E2/M1 = -1.1 \pm 0.4\%$ ,  $-1.5 \pm 0.2\%$ , [4],  $3.7 \pm 0.4\%$  [12] and  $-1.3 \pm 0.5\%$ . Some other calculations give:  $E2/M1 = -3.1\%$  [5],  $-4\%$  [13], and  $0\%$  [14]. These differences are a reflection of the fact that extraction of the  $E2/M1$  ratio from the large experimental background requires a theoretical model for both the  $\Delta$  resonance and the background, and the result one obtains is therefore sensitive to how the theoretical models are unitarized, and to how the background is described [5]. We expect that new, accurate data from CEBAF experiments, and new, more complete models of  $\pi$  photoproduction, will help to clarify the situation.

The value of the  $E2/M1$  which we obtain from our fit (at the resonance pole  $W_{tot} = M_{\Delta}$ ) is

$$E2/M1 = -1.46\%. \quad (1.1)$$

This is small and negative, in agreement with some of the results given above. This value was calculated from the  $\Delta$ -pole diagram only, and does not include any contributions from the background. The *total*  $E2/M1$  ratio, including background contributions, is  $-0.63$ .

### C. Low Energy Theorem

The low energy theorem (LET) was derived for the first time by Kroll and Ruderman [15] from an examination of the implications of gauge invariance in the framework of field theory. Later Fubini et al. [16], extended this theory by including the hypothesis of a partially conserved axial current (PCAC). In view of the LET, threshold pion production on the nucleon was considered to be well understood. According to the original LET prediction the threshold value of the electric dipole amplitude for  $\pi^0$  photoproduction from protons is

$$\begin{aligned} E_{0+}|_{LET} &= -\frac{eg_{\pi NN}\mu}{8\pi m^2} \left(1 - \frac{\mu}{2m}(3 + \kappa_p)\right) + \mathcal{O}\left(\frac{\mu}{m}\right)^3 \\ &= -\frac{2.3 \times 10^{-3}}{\mu} + \text{correction}, \end{aligned} \quad (1.2)$$

where  $\mu$  is the pion mass. However it was a big surprise when an analysis of the Saclay data [17] showed that the experimental threshold amplitude  $E_{0+}$  for  $\pi^0$  photoproduction was smaller than the prediction of LET by about a factor of five

$$E_{0+}|_{expt} = \frac{(-0.5 \pm 0.3) \times 10^{-3}}{\mu}. \quad (1.3)$$

The Mainz analysis [18] confirmed this result, and renewed interest in the LET. Possible flaws in the derivation of the LET due to final state interactions [19], corrections to the chiral perturbation expansion [20], or chiral symmetry breaking corrections [21–23], were proposed. A new contribution of order  $\mu/m$  (which arises from logarithmic singularities of some one-loop diagrams in the chiral perturbation expansion) was discovered [20], giving a corrected LET

$$\begin{aligned} E_{0+}|_{LET} &= -\frac{eg_{\pi NN}\mu}{8\pi m^2} \left[1 - \frac{\mu}{2m} \left(3 + \kappa_p + \frac{m^2}{8F_\pi^2}\right)\right] + \mathcal{O}\left(\frac{\mu}{m}\right)^3 \\ &= -\frac{1.4 \times 10^{-3}}{\mu} + \text{correction}, \end{aligned} \quad (1.4)$$

where  $F_\pi$  is the pion decay constant. Then, instead of extracting the low energy result from the differential cross section, Bernstein and Holstein [24] and Drechsel and Tiator [25] used the total cross section (which was not analyzed by the Mainz group) and obtained:

$$E_{0+} = \frac{(-2.0 \pm 0.2) \times 10^{-3}}{\mu}. \quad (1.5)$$

It is clear that the threshold value of  $E_{0+}$  will continue to be of interest, and that it may be a case where the chiral perturbation expansion is slow to converge.

The result we obtain for the electric dipole amplitude at threshold,

$$E_{0+} = \frac{-1.34 \times 10^{-3}}{\mu}, \quad (1.6)$$

is very close to the result (1.4).

### D. Unitarity

Symbolically, the unitarity statement can be written [see Eq. (2.14) below]

$$Im M_{\pi\gamma}^\alpha = -\rho_\pi M_{\pi\pi}^{\alpha*} M_{\pi\gamma}^\alpha - \rho_\gamma M_{\pi\gamma}^{\alpha*} M_{\gamma\gamma}^\alpha, \quad (1.7)$$

where  $M_{\pi\pi}^\alpha$ ,  $M_{\pi\gamma}^\alpha$ , and  $M_{\gamma\gamma}^\alpha$  are the  $\pi N$ , pion photoproduction, and compton scattering matrices for a state with quantum numbers  $\alpha$ , and  $\rho_\pi$  and  $\rho_\gamma$  are phase space factors for the  $\pi N$  and  $\gamma N$  intermediate states. In 1954 Watson [9] pointed out that the second term in Eq. (1.7) is very small because it contains no terms which are first order in  $e$  (the electric charge), and can therefore be neglected. Below the two pion production threshold, the phase of the pion photoproduction amplitude for a state  $\alpha$  will therefore be equal to the phase of  $\pi N$  scattering in the same channel. This statement can be explicitly written

$$M_{\pi\gamma}^\alpha = |M_{\pi\gamma}^\alpha| e^{i\delta_{\pi\pi}^\alpha}, \quad (1.8)$$

where  $\delta_{\pi\pi}^\alpha$  is the partial wave phase shift for  $\pi N$  scattering. The Watson statement (1.8), sometimes called the Watson theorem, will start breaking down above the two pion production threshold.

Unitarity was incorporated into models based on dispersion relations by Chew, Goldberger, Low, and Nambu (CGLN) [1] and by Fubini, Nambu, and Wataghin [26]. Early models based on effective lagrangians were not unitary [3,27] but were later unitarized [3,28,29]. As pointed out by Araki and Afnan [30] quark models based on effective lagrangians are hard to interpret because it is difficult to establish the connection between the coupling constants in the lagrangian and observed interaction strengths.

The importance of unitarity was recently pointed out by Nozawa, Blankleider and Lee (BNL) [5], who claim that it is impossible to fit the  $M_{1+}$  and  $E_{1+}$  multipoles with a nonunitarity model. The same observation was made by Wittman, Davidson, and Mukhopadhyay [4] who also showed that the result for these amplitudes can be improved by unitarizing the model. These models are unitary

because they use a covariant integral equation with solutions which are automatically unitary. Ohta and Tanabe [12] and Yang [13] use an integral equation with a separable  $\pi N$  potential. While their result is unitary, the value of  $E_{0+}$  at threshold is sensitive to the particular separable expansion used, and they are not able to determine a unique value of  $E_{0+}$ . To obtain a unitary amplitude, Lee and his collaborators [5,31] use a reduction of the Bethe-Salpeter equation in which both of the intermediate particles are on mass-shell, but they do not use this prescription in the calculation of renormalization constants, losing consistency.

Our model uses a relativistic wave equation in which the intermediate state pion is on shell and the intermediate state nucleon is off shell. This is consistent with the  $\pi N$  model previously developed [7]. In our model, the same equations are used to calculate both the scattering amplitude and the renormalized coupling constants, insuring that the renormalization of the propagators and vertices is carried out in a manner that is consistent with unitarity.

### E. Gauge Invariance

It has been known since 1954, when Kroll and Ruderman (KR) [15] wrote their well-known paper on pion photoproduction, that the momentum dependence of the pseudovector  $\pi NN$  coupling requires introduction of an interaction current (the famous Kroll-Ruderman term) in order to satisfy gauge invariance. More recently, using minimal substitution, Ohta [32] and Naus, Koch, and Friar [33] obtained a gauge invariant set of Born terms which included form factors. Antwerpen and Afnan [34] extended this theory to the treatment of pion photoproduction with final state interactions, but have not obtained numerical results. In their approach they require the dressed  $\pi NN$  vertex to be gauge invariant by itself. The NBL model [5,31] also includes final state interactions, and satisfies gauge invariance by restricting both of the intermediate particles to their mass shell.

In this paper we apply the method originally introduced by Gross and Riska [35]. They show how the electromagnetic coupling to any two body system described by a relativistic two body equation (such as the Bethe-Salpeter equation or the Gross equation [7,36]), will always conserve current provided the following three conditions are met: (i) the electromagnetic currents for the interacting off-shell nucleon and mesons satisfy the appropriate Ward-Takahashi (WT) identities; (ii) the interacting incoming and outgoing two body system satisfy the same two body relativistic equation (with the same interaction kernel); and (iii) the exchange (or interaction) current is built up from the relativistic kernel by coupling the virtual photon to all possible places in the kernel. This method

works even in the presence of strong form factors for the off shell nucleon; in this case it is only necessary to modify the structure of the off-shell  $\gamma NN$  vertex so that it satisfies the a WT identity with dressed propagators (as discussed in Sec. IV).

Using this method, it is possible to construct a gauge invariant theory even when particles are off shell, but gauge invariance is achieved only through cancellations among all of the diagrams in the theory. To prove gauge invariance (as is done in Sec. II), we use the WT identities, the relativistic wave equation satisfied by the  $\pi N$  system, and must be careful to introduce interaction currents (in addition to the well-known KR interaction current) which arise from the momentum dependence of the interaction kernel.

### F. Results

The basic features of our  $\pi N$  scattering model are already well described in Ref. [7], and the modifications of this original model are described in Sec. III. New numerical results for pion nucleon  $S$ ,  $P$ , and  $D$  wave phase shifts and inelasticities are shown in Figs. 3-8 and the new parameters are given in Table I. (The interested reader may compare these with the corresponding Table I and Figs. 7-13 in Ref. [7].)

Our fit to the pion-nucleon phase shifts and inelasticities are very good, with a major improvement (over the original model [7]) in the  $S_{31}$  channel (see Fig. 3) which improves the scattering length. The new values of the scattering lengths are:

$$\begin{aligned}\mu a_- &= 0.07 \\ \mu a_+ &= -0.05\end{aligned}\tag{1.9}$$

which is very close to the experimental results [37]:

$$\begin{aligned}\mu a_-|_{\text{expt}} &= 0.085 \pm 0.01 \\ \mu a_+|_{\text{expt}} &= -0.02 \pm 0.02.\end{aligned}\tag{1.10}$$

Fig. 4 shows fits to the the  $P_{11}$  and  $P_{31}$  phase shifts. In the  $P_{11}$  channel the zero appears at 101 MeV pion lab kinetic energy. The fits to  $P_{33}$ ,  $P_{31}$  and  $D_{13}$  channels shown in Fig. 5 and Fig. 6 are very good. Because of our approximation for the inelastic channels, our fits to the  $P_{11}$  and  $D_{13}$  inelasticity parameters are not very good especially at the higher energy.

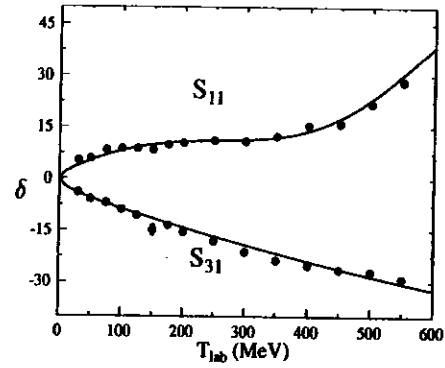


Figure 3: Fits to the  $S_{11}$  and  $S_{31}$  phase shifts. The black dots are the Arndt phase shifts.

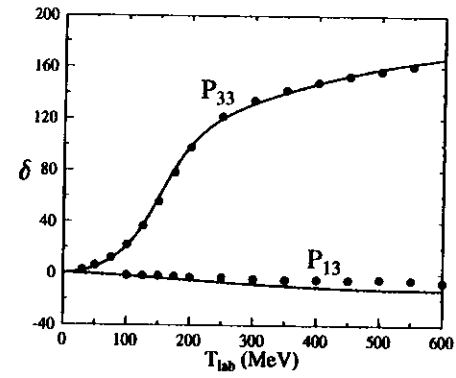


Figure 5: Fits to the  $P_{13}$  and  $P_{33}$  phase shifts.

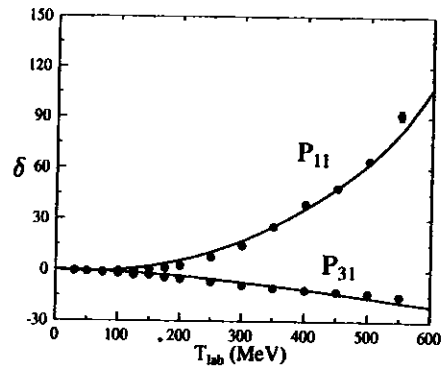


Figure 4: Fits to the  $P_{11}$  and  $P_{31}$  phase shifts.

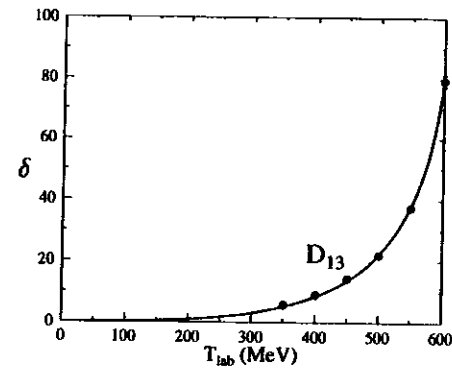


Figure 6: Fit to the  $D_{13}$  phase shifts.

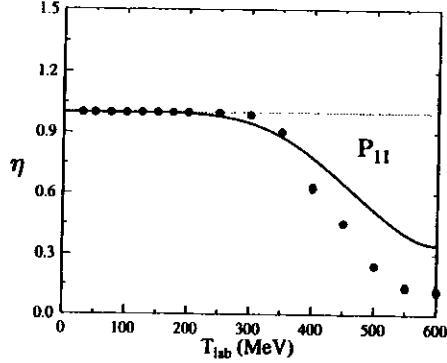


Figure 7: The  $P_{11}$  inelasticity parameter.

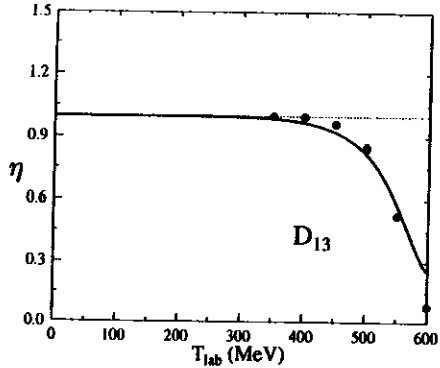


Figure 8: The  $D_{13}$  inelasticity parameter.

The 13 parameters given in boldface in Table I were adjusted during the fits. The table also includes several parameters which were determined by the fit or fixed by consistency requirements. All of these parameters, except for the new inelasticity parameters  $g'_{1B}$  and  $g'_{2B}$  (where  $B = \{N^*, D\}$ , see Sec. III), have been discussed in detail in Ref. [7]. We choose  $g'_{2B} = 0$ . The inelasticities of the  $N^*$  and  $D_{13}$  are described approximately by introducing a  $\sigma^*N$  channel, where  $\sigma^*$  is a (fictitious) scalar particle with a mass equal to two pion masses, or 278 MeV. The mass of the  $\sigma^*$  was chosen so that the  $\sigma^*N$  threshold would coincide exactly with the  $\pi\pi N$  threshold, which seems to be critical to a good description of the inelasticity.

The numerical results for the multipole amplitudes for pion photoproduction from a proton are shown in Figs. 9–21 and the new parameters which describe the coupling of the photon to the nucleon (and meson) resonances are given in Table II. The experimental results shown in the figures come from the VPI interactive SAID program of Arndt and Roper [38]. The amplitudes are given in units of  $(\text{fm}) \times 10^{-3}$ . The precise definitions of the parameters shown in Table II are given in Sec. IV; those in boldface were adjusted during the fit.

The parameters  $g_{1B}$  and  $g_{2B}$  (where  $B = \{N^*, \Delta, D\}$ ) describe the  $\gamma NB$  couplings (there are two independent forms for each coupling, see Sec. IV), the products  $g_{v\pi\gamma}g_{vNN}$  (where  $v = \{\rho, \omega\}$ ) are the strengths of the  $\rho\pi\gamma$  and  $\omega\pi\gamma$  couplings (the fit can determine the product of these factors only), and the  $f_{vNN}/g_{vNN}$  are the ratio of the tensor ( $f_{vNN}$ ) to vector ( $g_{vNN}$ ) strengths of the  $\rho NN$  and  $\omega NN$  couplings. The  $f_{\rho NN}/g_{\rho NN}$  value given in Table II was taken from the  $NN$  Model IA of Ref. [36], while the  $f_{\omega NN}/g_{\omega NN}$  was adjusted to improve the fit.

Because of our choice of spin 3/2 propagator and our approximation scheme which sets the crossed  $\Delta$  and  $D_{13}$  pole terms to be zero, the  $\Delta$  and the  $D_{13}$  only contribute to the  $j = 3/2$  channels. It is therefore convenient to describe our fits to the  $j = 1/2$  and  $j = 3/2$  channels separately.

We begin with the  $j = 1/2$  channels, shown in Figs. 9–12. These channels are driven by the nucleon and  $N^*$  poles and crossed poles, and the  $\pi$ ,  $\omega$  and  $\rho$  exchange terms (see Sec. IV for details). These driving terms depend on five adjustable parameters: two  $\gamma NN^*$  couplings, denoted by  $g_{1N^*}$  and  $g_{2N^*}$ , the  $\rho\pi\gamma$  and  $\omega\pi\gamma$  couplings multiplied by the  $\rho NN$  and  $\omega NN$  couplings, denoted by  $g_{\rho\pi\gamma}g_{\rho NN}$  and  $g_{\omega\pi\gamma}g_{\omega NN}$  and the  $\omega$  anomalous magnetic moment coupling  $\kappa_\omega = f_{\omega NN}/g_{\omega NN}$ . To show how the total result is built up from individual contributions, the curves in the figures show the result when the kernel (i) includes only the direct nucleon pole term, the crossed nucleon pole, the pion exchange pole, and all the interaction currents associated with the nucleon (the dotted



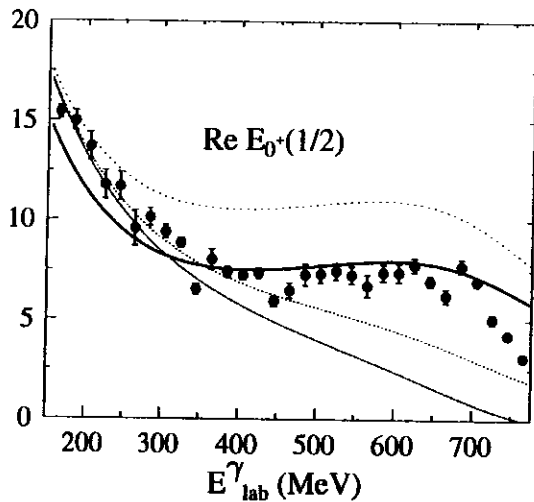


Figure 9: Fit to the real part of  $E_{0+}(1/2)$  amplitude. The individual contributions are discussed in the text.

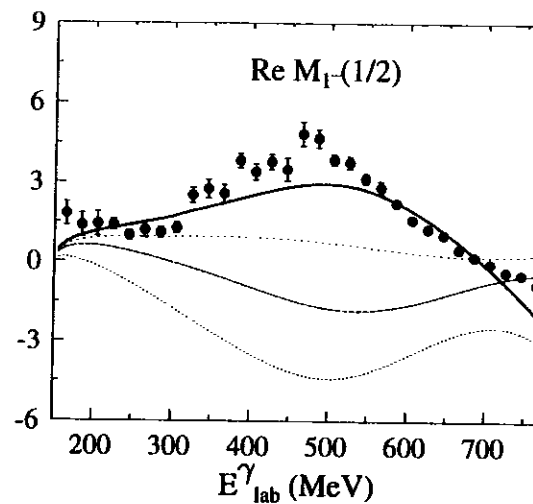


Figure 11: Fit to the real part of  $M_{1-}(1/2)$  amplitude.

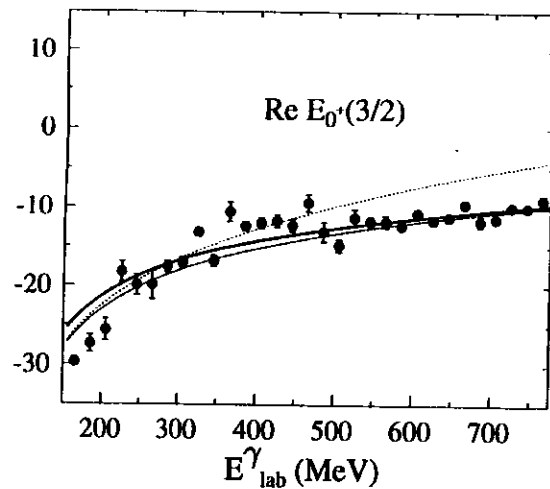


Figure 10: Fit to the real part of the  $E_{0+}(3/2)$  amplitude. The  $\rho$  exchange pole does not contribute to this channel, and the  $N^*$  gives a small contribution (the dashed line nearly overlaps the solid line).

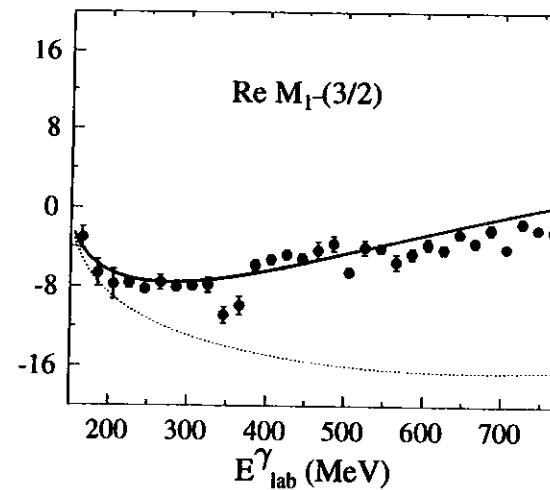


Figure 12: Fit to the real part of the  $M_{1-}(3/2)$  amplitude. The  $\rho$  exchange pole does not contribute to this channel, and the  $N^*$  gives a very small contribution (the dashed line overlaps the solid line).

line), (ii) the terms in (i) plus the  $\omega$  exchange pole (the dashed line), (iii) the terms in (ii) plus  $\rho$  exchange pole (the dotted line, with wider space between dots), and finally (iv) the total result, which includes the terms in (iii) plus the  $N^*$  contributions (the solid line). Since all contributions add non-linearly, it is difficult to extract the separate contributions from the figures.

Our fits to both the real and imaginary parts of the  $j = 1/2$  multipole amplitudes are very good. In the  $S_{11}$   $\pi N$  channel (Fig. 9) there is a small peak near 730 MeV that we can not describe. This peak is associated with  $\eta$  production, not included in our model. This  $\eta$  production also contributes to the  $S_{31}$  channel (Fig. 10) at high energy.

Before we discuss the fits to the  $j = 3/2$  channels, we wish to point out that the  $E_{0+}(1/2)$  and  $M_{1-}(1/2)$  amplitudes, shown in Figs. 9 and 11, are particularly sensitive to all of the individual contributions. In contrast, the  $\rho$  exchange is isoscalar and does not contribute to the  $I = 3/2$  amplitudes (the  $E_{0+}(3/2)$  and  $M_{1-}(3/2)$ , shown in Figs. 10 and 12), and the Roper also gives only a very small contribution to these  $I = 3/2$  channels (the dashed line overlaps, or almost overlaps, the solid line). The  $\omega$  and  $\rho$  exchange contribution are very important to a description of the two  $I = 1/2$  amplitudes. The Roper is also very significant, especially in the  $M_{1-}(1/2)$  amplitude, which cannot be fit without it. The  $M_{1-}(3/2)$  amplitude (Fig. 12) depends very much on the omega, and could not be fit without varying the  $(f_{\omega NN}/g_{\omega NN})$  coupling. The small value of  $(f_{\omega NN}/g_{\omega NN})$  from one the boson exchange models [36] did not work.

The  $j = 3/2$  channels, shown in Figs. 13-16, are driven by the direct spin 3/2 resonance poles (from the  $\Delta$  and  $D_{13}$ ), the crossed  $N$  and  $N^*$  pole diagrams, and the  $\pi$ ,  $\rho$ , and  $\omega$  exchange diagrams. As before, the  $\rho$  exchange pole does not contribute to the  $I = 3/2$  amplitudes, so the contributions shown in Figs. 13 and 14 include (i) contributions from the nucleon and pion only (dotted line as above), (ii) terms in (i) plus the omega exchange pole (line with short dashes, as above), (iii) the terms in (ii) plus the  $N^*$  contributions (the line with longer dashes) and (iv) the total result, including the  $\Delta$  pole terms (solid line). For the  $I = 1/2$  amplitudes, the widely spaced dotted line includes terms in (ii) above plus the  $\rho$  exchange (as in the  $j = 1/2$  cases), the line with longer dashes adds the  $N^*$  contributions, and the solid line is the total, including the  $D_{13}$ . All of the parameters for the crossed and exchange diagrams were already determined by the  $j = 1/2$  fit. The direct  $\Delta$  pole, which contributes only to the  $P_{33}$  final state (Figs. 13 and 14), requires two new parameters (the couplings  $g_{1\Delta}$  and  $g_{2\Delta}$ ), and the direct  $D_{13}$  pole, which contributes only to the  $D_{13}$  final state (Figs. 15 and 16), requires two more (the couplings  $g_{1D}$  and  $g_{2D}$ ). The values of the  $\gamma N \Delta$  couplings which we obtain are within range of other calculations [39] which use

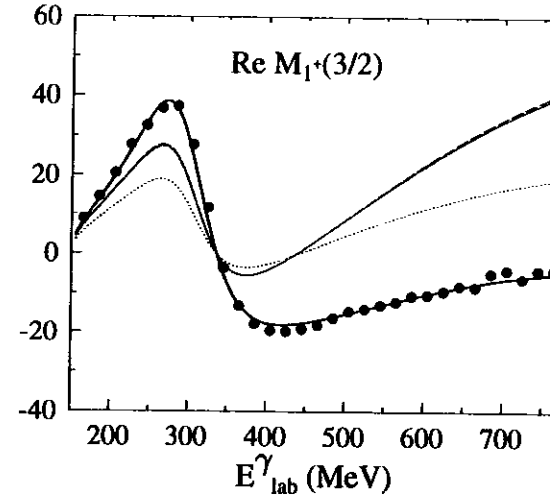


Figure 13: Fit to the real part of  $M_{1+}(3/2)$  amplitude. The individual contributions are discussed in the text. The  $N^*$  contribution is very small, and the  $\rho$  does not contribute.

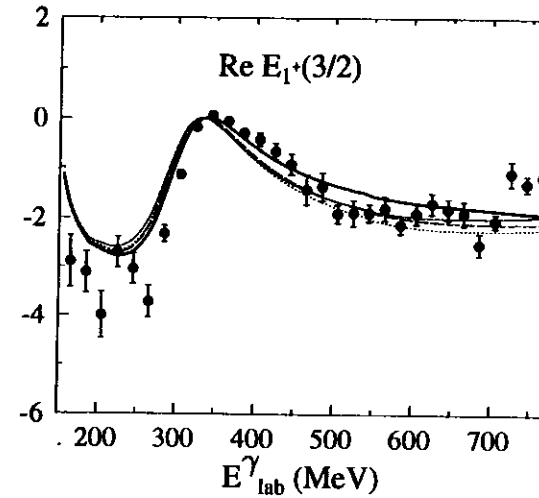


Figure 14: Fit to the real part of the  $E_{1+}(3/2)$  amplitude. See the caption to Fig. 13.

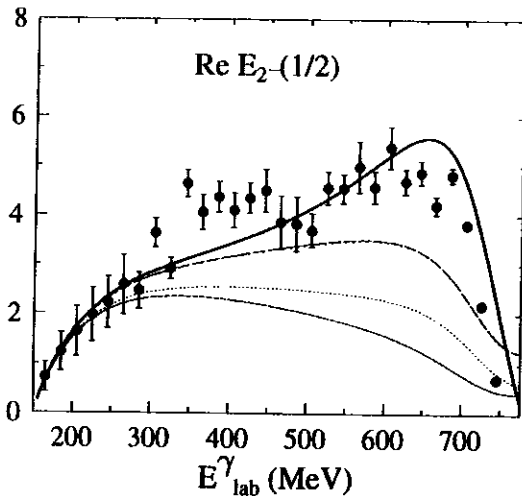


Figure 15: Fit to the real part of  $E_{2-}(1/2)$  amplitude. The individual contributions are discussed in the text. The  $N^*$  contribution is very small (as indicated by the overlap of the long-dashed line and the widely spaced dotted line).

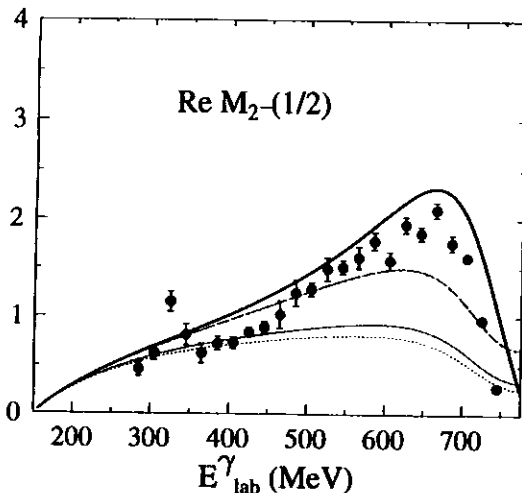


Figure 16: Fit to the real part of the  $M_{2-}(1/2)$  amplitude. See the caption to Fig. 15.

the Rarita Schwinger propagator to describe the spin  $3/2$  resonances.

All of the  $j = 3/2$  amplitudes are fit reasonably well by the model. The contribution of the  $N^*$  to all of these amplitudes is very small (as indicated by the near overlap of the lines with short and long dashes in Figs. 13 and 14 and the lines with widely spaced dots and long dashes in Figs. 15 and 16). Note that the rho exchange pole plays an important role in the  $E_{2-}(1/2)$  and  $M_{2-}(1/2)$  amplitudes (Figs. 15 and 16).

From the results shown in Figs. 13 and 14 we calculated the ratio of  $E_{1+}(3/2)$  and  $M_{1+}(3/2)$  at the peak of the  $\Delta$  resonance, and found that the value from only the dressed  $\Delta$  contribution is about  $-1.46\%$ .

Finally, Figs. 17 – 20 show the comparison of our calculation (solid lines) to the VPI analysis [38] (dashed lines). The black dots and open triangles are the real and imaginary parts of the amplitudes, respectively. The agreement between the two calculations is good.

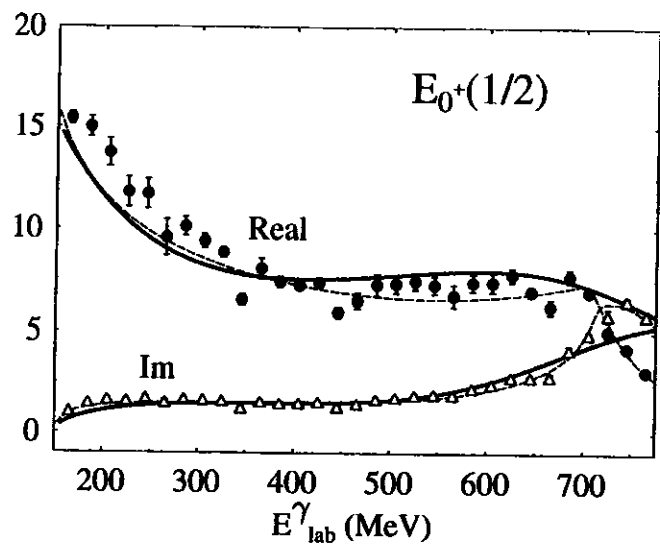
### G. Form Factors

Some form factors are needed to insure that the solutions of the integral equation exist, or alternatively, to cut off the integrals over the  $\pi N$  and (the inelastic)  $\sigma^* N$  loops which appear in the solution. These form factors cannot depend on the pion mass, as is usually done in pion exchange models, because the pion is on-shell. Anticipating the extension of this model to the description of the electro-production of pions, where a gauge invariant treatment of electromagnetic interactions is possible following the procedure introduced in Ref. [35], we choose to make the form factors depend only on the off-shell nucleon mass. By extension, and to improve the fits, we also introduce form factors for the baryon resonances. These form factors are identified with the baryon itself; each baryon has a universal form factor which will be used for that baryon, wherever it appears in the calculation. We also require all form factors to be zero in the space like region (when  $p^2 < 0$ ).

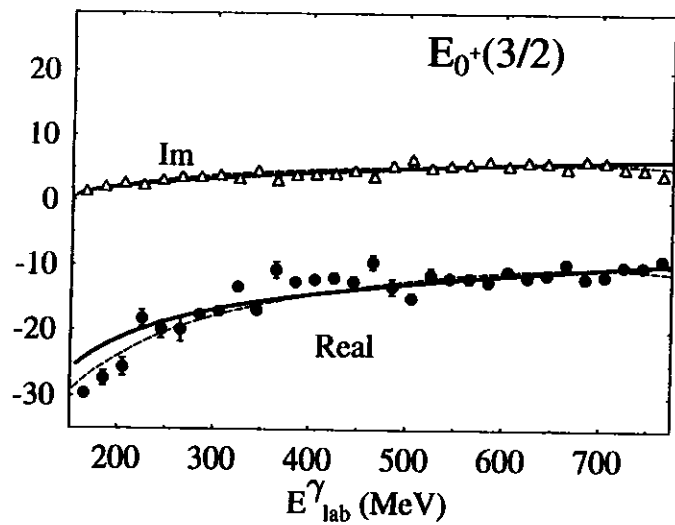
The specific form of the baryon form factors used in this paper, which are different from those used in Ref. [7], is

$$f_B(p^2) = \left[ \frac{(\Lambda_B^2 - m_B^2)^2}{(\Lambda_B^2 - m_B^2)^2 + (m_B^2 - p^2)^2} \right]^2 \left[ \frac{p^4 (\mu^4 + (\mu^2 + m_B^2)^2)}{m_B^4 (\mu^4 + (\mu^2 + p^2)^2)} \right] \theta(p^2), \quad (1.11)$$

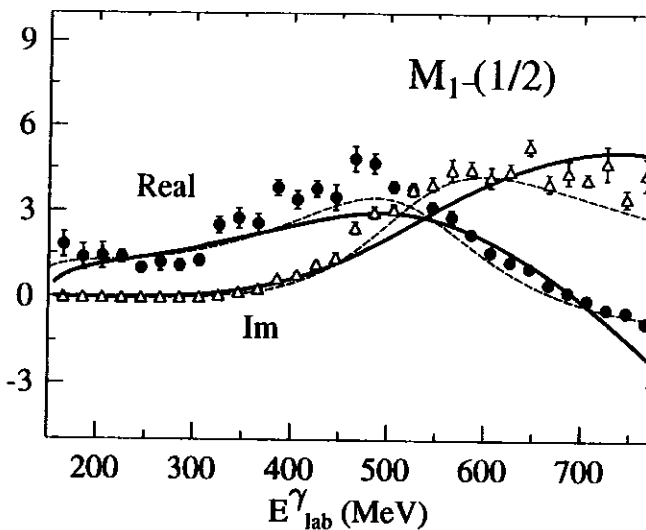
where  $m_B = m$  for  $B = \{N, \Delta, D_{13}\}$ ,  $m_B = m^*$  (the Roper mass) for the Roper, the form factor masses  $\Lambda_B$  were allowed to vary during the fit, and the theta function is introduced to insure that this form factor is zero for  $p^2 < 0$ . Note



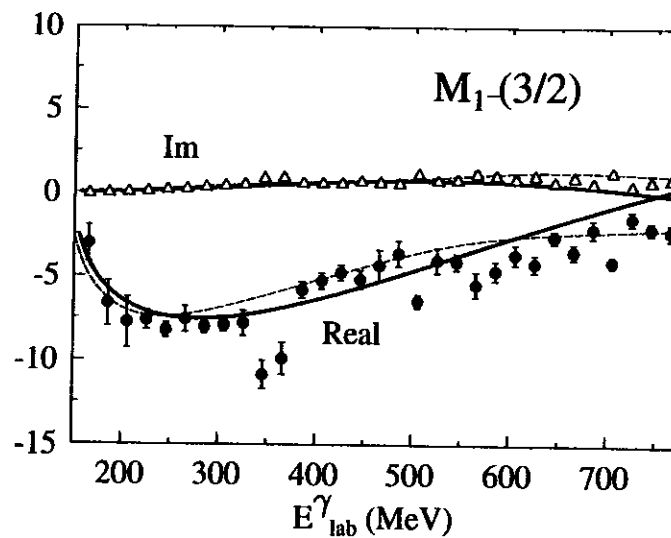
(a)



(b)



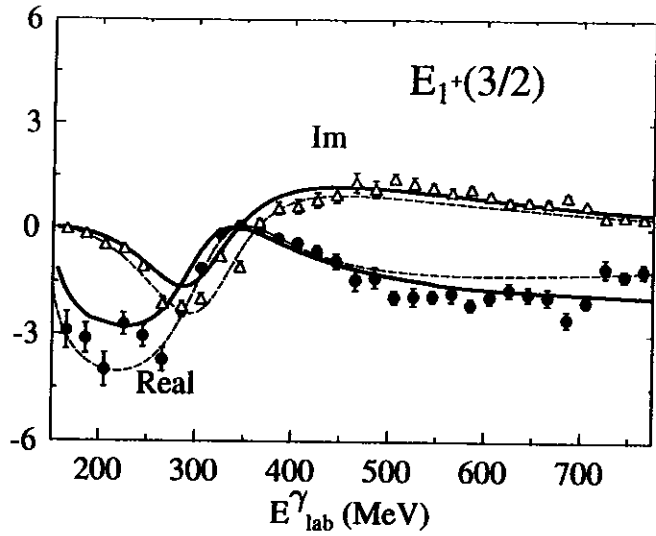
(a)



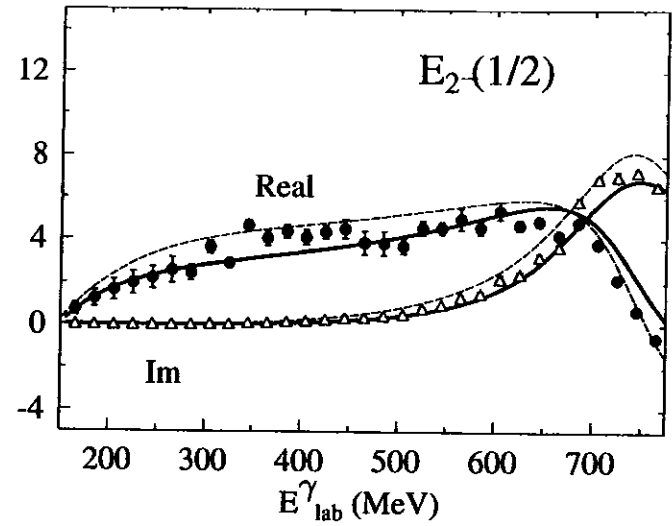
(b)

Figure 17: Comparison of our  $E_{0+}(1/2)$  and  $(3/2)$  to SAID analysis. See the discussion in the text.

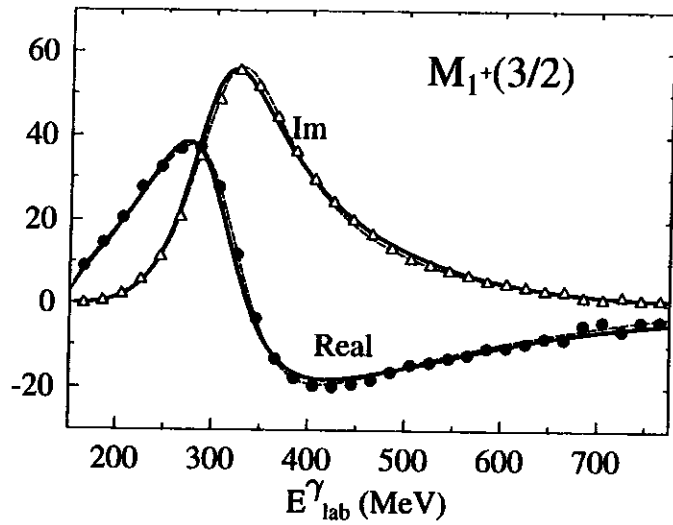
Figure 18: Comparison of our  $M_{1-}(1/2)$  and  $(3/2)$  amplitudes.



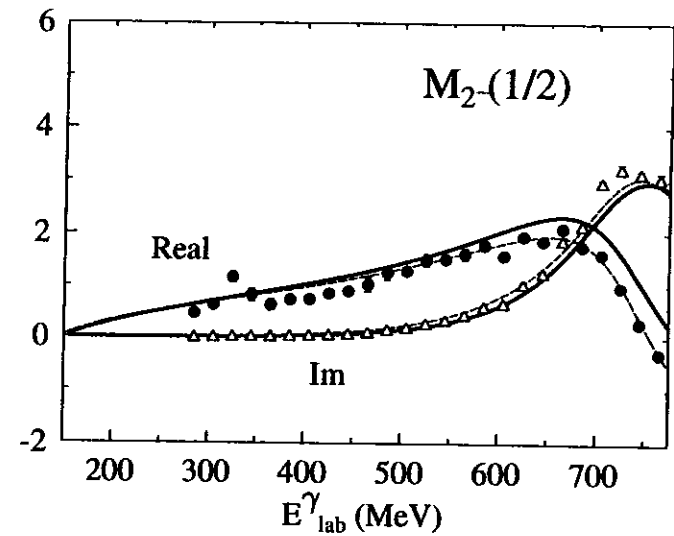
(a)



(a)



(b)



(b)

Figure 19: Comparison of our  $E_{1+}(3/2)$  and  $M_{1+}(3/2)$  amplitudes.

Figure 20: Comparison of our  $E_{2-}(1/2)$  and  $M_{2-}(1/2)$  amplitudes.

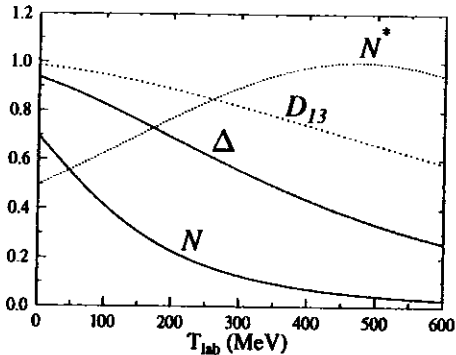


Figure 21: Form factors for the nucleon (solid line), Roper (dotted line),  $\Delta$  (dashed line), and  $D_{13}$  (widely space dotted line) as a function of  $T_{\text{lab}}$ .

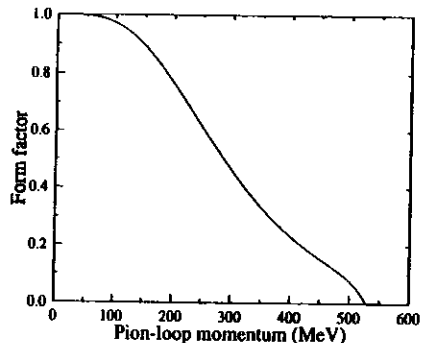


Figure 22: Form factor of the nucleon plotted as a function of the pion loop momentum.

that the maximum value of the first factor is unity at  $p^2 = m_B^2$ , and that this term peaks at  $p^2 = m^2$  for the nucleon,  $\Delta$ , and  $D_{13}$  form factors, while it peaks at  $p^2 = m^{*2}$  for the  $N^*$  form factor. Unfortunately, our results are sensitive to the form factors, which are purely phenomenological.

When the form factors accompany the intermediate baryon in the direct baryon pole terms, the virtual mass (squared) is simply

$$p^2 = m^2 + \mu^2 + 2m(T_{\text{lab}} + \mu) , \quad (1.12)$$

and the four baryon form factors are plotted versus  $T_{\text{lab}}$  in Fig. 21. When the nucleon form factor accompanies a virtual nucleon in a  $\pi N$  loop, its mass (squared) is

$$p^2 = W^2 + \mu^2 - 2W\omega(k) , \quad (1.13)$$

where  $k$  is the magnitude of the pion three-momentum in the loop, and  $\omega(k) = \sqrt{\mu^2 + k^2}$ . The nucleon form factor is plotted versus  $k$  for a fixed  $W = m + \mu$  in Fig. 22. We emphasize that the *same* nucleon form factor is shown in both figures; only the variable on which it depends has been changed. Note that (because of the theta function) the nucleon form factor is zero beyond  $k \simeq 525$  MeV, cutting off the loop integral at this momentum. [However, a more gentle cutoff, such as the ones used in Ref. [7], does not alter the results significantly.]

## H. Conclusions

The following conclusions can be drawn from the present work:

(i) A relativistic resonance model of pion-photoproduction, fully consistent with the  $\pi N$  scattering model which defines the final state interactions, has been found to give a good description of the process up to 750 photon laboratory energy. The model is covariant, satisfies unitarity up to first order in the electric charge  $e$ , and is gauge invariant to all orders. The simplicity and consistency of the two models means that they can be used as a basis for a treatment of the coupled  $NN \leftrightarrow \pi NN$  system, and its electromagnetic extension to  $\gamma NN$  and  $\gamma\pi NN$ .

(ii) The dressed  $\Delta$  contribution gives a ratio of  $E2/M1 = -1.46\%$  at the  $\Delta$  pole, implying that the  $\Delta$  is not purely an  $S$  state, but contains a  $D$  state admixture. This result shows that the tensor interaction between quarks should not be neglected.

(iii) The threshold value of the electric dipole moment for  $\pi_0$  photoproduction from protons is  $E_{0+} = -1.34 \times 10^{-3}/\mu$ , which is in agreement with the recent value predicted by chiral perturbation theory.

## II. GENERAL THEORY

In this section the relativistic equation for the pion-photoproduction scattering matrix is presented, and we show that the theory is covariant, gauge invariant and satisfies unitarity.

### A. Integral Equations

The Bethe-Salpeter equation for pion-photoproduction can be written in two equivalent ways. Keeping the terms lowest order in  $\epsilon$  only, and suppressing all the Dirac and isospin indices gives

$$\begin{aligned} M_{\pi\gamma}(k', q, P) &= V_{\pi\gamma}(k', q, P) + i \int \frac{d^4 k''}{(2\pi)^4} V_{\pi\pi}(k', k'', P) G(k'', P) M_{\pi\gamma}(k'', q, P) \\ &= V_{\pi\gamma}(k', q, P) + i \int \frac{d^4 k''}{(2\pi)^4} M_{\pi\pi}(k', k'', P) G(k'', P) V_{\pi\gamma}(k'', q, P), \end{aligned} \quad (2.1)$$

where  $V_{\pi\gamma}(k', q, P)$  and  $V_{\pi\pi}(k', k'', P)$  are the driving terms for the  $\gamma\pi$  and  $\pi\pi$  sectors, respectively, and  $G(k'', P)$  is the two-body  $\pi N$  propagator. The four-momenta of the incoming, outgoing, and intermediate nucleon are  $p$ ,  $p'$  and  $p''$ , of the outgoing, and intermediate pion are  $k'$ , and  $k''$ , and of the incoming photon is  $q$ , so that  $P = p + q = p' + k' = p'' + k''$  is the total four-momentum. The equivalence of the two forms of Eq. (2.1) follows from their Born series, which is identical. To see this, it is necessary to use the equations for the  $\pi N$  scattering amplitude, which are

$$\begin{aligned} M_{\pi\pi}(k', k, P) &= V_{\pi\pi}(k', k, P) + i \int \frac{d^4 k''}{(2\pi)^4} V_{\pi\pi}(k', k'', P) G(k'', P) M_{\pi\pi}(k'', k, P) \\ &= V_{\pi\pi}(k', k, P) + i \int \frac{d^4 k''}{(2\pi)^4} M_{\pi\pi}(k', k'', P) G(k'', P) V_{\pi\pi}(k'', k, P). \end{aligned} \quad (2.2)$$

In Ref. [7] we have shown that pion nucleon scattering is well described by a relativistic equation obtained from Eq. (2.2) by putting the intermediate pion on mass-shell. To be consistent with this description of  $\pi N$  scattering, we also put the intermediate pion on the mass-shell in the  $\gamma N$  Eqs. (2.1). [The only place that the pion will be off-shell is in one of the pion pole driving terms, which

is needed to satisfy gauge invariance, as discussed below.] If the pion is put on-shell, the Eq. (2.1) becomes

$$\begin{aligned} M_{\pi\gamma}(k', q, P) &= V_{\pi\gamma}(k', q, P) \\ &\quad - \int \frac{d^3 k''}{(2\pi)^3 2\omega_{k''}} V_{\pi\pi}(k', k'', P) S_N(p'') M_{\pi\gamma}(k'', q, P) \\ &= V_{\pi\gamma}(k', q, P) \\ &\quad - \int \frac{d^3 k''}{(2\pi)^3 2\omega_{k''}} M_{\pi\pi}(k', k'', P) S_N(p'') V_{\pi\gamma}(k'', q, P), \end{aligned} \quad (2.3)$$

where  $\omega_{k''} = \sqrt{\mu^2 + \mathbf{k}''^2}$  is the on-shell pion energy, and

$$S_N(p'') = \frac{1}{m - \not{p}'' - i\epsilon} \quad (2.4)$$

is the nucleon propagator, and  $\mu$  and  $m$  are the pion and the nucleon masses.

The equations are regularized by adding a form factor,  $f_N(p^2)$ , to damp the high momentum behavior of the off-shell nucleon of momentum  $p$ . The Eqs. (2.3) include these form factors in the interaction kernel  $V$ . Alternatively, it is sometimes convenient (particularly in our discussion of gauge invariance below) to move these form factors from the kernel to the propagator. To this end we can introduce *reduced* amplitudes and *damped* propagators as follows:

$$\begin{aligned} V(k', k, P) &= f_N[(P - k')^2] \tilde{V}(k', k, P) f_N[(P - k)^2] \\ M(k', k, P) &= f_N[(P - k')^2] \tilde{M}(k', k, P) f_N[(P - k)^2] \\ \tilde{S}_N(p'') &= f_N^2(p''^2) S_N(p''). \end{aligned} \quad (2.5)$$

The symbol  $\tilde{M}$  will usually denote the reduced amplitude  $M$  (the amplitude  $M$  with the form factors removed) and  $\tilde{S}$  the damped propagator with the (square of the) nucleon form factor added. It is easy to verify that the reduced amplitudes satisfy the same equations, but with damped propagators substituted for "bare" propagators.

We will have occasion to use the fact that the pion nucleon scattering matrix  $M_{\pi\pi}(k', k, P)$  can be written in the following form (see Ref. [7]):

$$M_{\pi\pi}(k', k, P) = M_{c\pi\pi}(k', k, P) + \sum_B \Gamma_B(k', P) G_B(P) \bar{\Gamma}_B(k, P) \quad (2.6)$$

where the sum is over baryons  $B$  in the set  $\{N, N^*, \Delta, D_{13}\}$ ,  $M_{c\pi\pi}(k', k, P)$  is the infinite sum of iterated contact diagrams,  $\Gamma_B(k, P)$  is the dressed vertex for

baryon  $B$ , and  $G_B(P)$  is the dressed baryon propagator. (The definition of the Dirac conjugate,  $\bar{\Gamma}_B$ , will be given in the next subsection; note that it, and the notation used in Eq. (2.6), differs from that given in Ref. [7]. For a complete review of our notational conventions, see Appendix A.)

The integral equations (2.3) are manifestly covariant. This is guaranteed by the covariance of the volume integration,

$$\int \frac{d^3k}{2\omega_k} = \int d^4k \delta_+(\mu^2 - k^2). \quad (2.7)$$

Furthermore, these equations automatically give a solution which satisfies unitarity to order  $e$  (the Watson theorem), as we show in the next subsection.

## B. Unitarity

The proof of unitarity is very similar to the one given in Ref. [36] for  $NN$  scattering. First, we write Eq. (2.3), and a similar one for  $\pi + N \rightarrow \gamma + N$  (pion photoabsorption) in the following compact form

$$\begin{aligned} M_{\pi\gamma} &= V_{\pi\gamma} - \int V_{\pi\pi} S M_{\pi\gamma} & (a) \\ M_{\gamma\pi} &= V_{\gamma\pi} - \int V_{\gamma\pi} S M_{\pi\pi} & (b) \end{aligned} \quad (2.8)$$

where  $M_{\pi\gamma}$ ,  $M_{\gamma\pi}$ , and  $M_{\pi\pi}$  are the scattering matrices for photoproduction, photoabsorption, and pion nucleon scattering, and  $V_{\pi\gamma}$ ,  $V_{\gamma\pi}$ , and  $V_{\pi\pi}$  are the driving terms (kernels) for photoproduction, photoabsorption, and  $\pi N$  scattering. The Dirac conjugate of the photoproduction kernel is the kernel for photoabsorption, but the  $\pi N$  kernel is self conjugate:

$$\begin{aligned} \bar{V}_{\pi\gamma}(k, q, P) &= \gamma_0 V_{\pi\gamma}^\dagger(k, q, P) \gamma_0 = V_{\gamma\pi}(q, k, P) \\ \bar{V}_{\pi\pi}(k', k, P) &= \gamma_0 V_{\pi\pi}^\dagger(k', k, P) \gamma_0 = V_{\pi\pi}(k, k', P). \end{aligned} \quad (2.9)$$

Taking the Dirac conjugate of Eq. (2.8b), and using Eq. (2.9), we obtain

$$\bar{M}_{\gamma\pi} = V_{\pi\gamma} - \int \bar{M}_{\pi\pi} \bar{S} V_{\pi\gamma}. \quad (2.10)$$

Using Eq. (2.8a) to replace the  $V_{\pi\gamma}$  driving term under the integral in this equation gives the following nonlinear equation for  $\bar{M}_{\gamma\pi}$

$$\bar{M}_{\gamma\pi} = V_{\pi\gamma} - \int \bar{M}_{\pi\pi} \bar{S} M_{\pi\gamma} - \int \int \bar{M}_{\pi\pi} \bar{S} V_{\pi\pi} S M_{\pi\gamma}. \quad (2.11)$$

A second nonlinear equation can be obtained from Eq. (2.8a) by using the Dirac conjugate of the  $\pi N$  equation

$$\bar{M}_{\pi\pi} = V_{\pi\pi} - \int \bar{M}_{\pi\pi} \bar{S} V_{\pi\pi} \quad (2.12)$$

to replace the  $V_{\pi\pi}$  driving term under the integral

$$M_{\pi\gamma} = V_{\pi\gamma} - \int \bar{M}_{\pi\pi} S M_{\pi\gamma} - \int \int \bar{M}_{\pi\pi} \bar{S} V_{\pi\pi} S M_{\pi\gamma}. \quad (2.13)$$

Subtracting Eq. (2.11) from Eq. (2.13) gives the *elastic* unitarity condition

$$M_{\pi\gamma} - \bar{M}_{\gamma\pi} = - \int \bar{M}_{\pi\pi} (S - \bar{S}) M_{\pi\gamma}. \quad (2.14)$$

Using time reversal invariance, the Dirac conjugate  $\bar{M}_{\gamma\pi}$  can be related to the complex conjugate of  $M_{\pi\gamma}$ .

In each eigen-channel, the elastic unitarity condition (2.14) automatically implies that the pion photoproduction amplitude has the same phase as the  $\pi N$  scattering amplitude, which is a statement of the Watson theorem [9]. However, above the inelastic threshold, i.e. when the  $\pi\pi N$  intermediate states become physical, the driving terms in our equation become complex, the elastic unitarity condition no longer holds, and the Watson theorem no longer applies.

## C. Introduction to the model

In this section we prepare the way for a demonstration of gauge invariance by giving a brief introduction to our model of pion-photoproduction. A detailed discussion of the structure of the couplings and the definition of parameters will be deferred to Sec. III. Here we will limit the discussion to those points essential to the proof of gauge invariance.

Our amplitude for pion-photoproduction is given by the sum of the Born diagrams shown in Fig. 1 and their final state interactions, shown in Fig. 2. The Born diagrams 1(a), (b), (e2) and (e3) include (in principle) contributions from all of the resonances  $B$ , but the contributions of the  $\Delta$  and  $D_{13}$  to diagram 1(b) are zero in the approximation we employ. Furthermore, the  $\gamma NN^*$ ,  $\gamma N\Delta$ ,  $\gamma ND_{13}$ ,  $\rho\pi\gamma$ , and  $\omega\pi\gamma$  couplings are all separately gauge invariant, and hence



the contributions of the baryon resonances to the diagrams (a) and (b), and of the  $\rho$  and  $\omega$  to diagram (c), can be ignored in the proof of gauge invariance, and will not be discussed further here. Diagrams 1(e3) and (f) are interaction currents which arise because of the momentum dependence of the elementary  $\pi N$  contact interaction and the  $\pi NN$ ,  $\pi N\Delta$ , and  $\pi ND_{13}$  couplings. In our model the  $\pi NN^*$  coupling does not depend on the momentum, and hence the Roper makes no contribution to diagram (e3).

Note that dressed vertices are needed in diagrams (b), (c), (e), and (f) because final state interactions cannot describe any  $\pi N$  interactions which take place *before* the photon is absorbed. Interactions which take place *after* the photon is absorbed are part of the final state interactions, and hence diagram (a) must contain only the bare vertex in order to avoid double counting.

The interaction kernel obtained from the Born diagrams in Fig. 1 has the form

$$\tilde{V}_{\pi\gamma}(k', q, P) = -ie \epsilon_\mu \tilde{J}^{i\mu}(k', q, P), \quad (2.15)$$

where  $\epsilon_\mu$  is the polarization vector of the incoming photon,  $i$  is the isospin of the outgoing pion, and we remove the overall factor of  $e$  so that all currents will not include this factor. The reduced current  $\tilde{J}^{i\mu}$  for the diagrams (a)–(d), including *nucleons only*, is

$$\begin{aligned} (\tilde{J}^{i\mu})_{a-d}(k', q, P) = & \tau_i \tilde{\Gamma}_{N0}(k', P) \tilde{S}_N(P) \tilde{j}_N^\mu(P, p) \\ & + \tilde{j}_N^\mu(p', p - k') \tilde{S}_N(p - k') \tilde{\Gamma}_N(k', p) \tau_i \\ & + \tilde{j}_\pi^{ij\mu}(k', k' - q) \tau_j \tilde{\Delta}(k' - q) \tilde{\Gamma}_N(k' - q, p) + \tilde{J}_{IN}^\mu(q), \end{aligned} \quad (2.16)$$

where  $\tilde{\Gamma}_N(k', p)$  is the reduced *dressed*  $\pi NN$  vertex for an outgoing pion with four-momentum  $k'$ ,  $\tilde{\Gamma}_{N0}(k', P)$  is the reduced *bare*  $\pi NN$  vertex,  $\tilde{\Delta}$  is the damped pion propagator,  $\tilde{j}_N^\mu(p', p)$  and  $\tilde{j}_\pi^{ij\mu}(k', k)$  are the reduced  $\gamma NN$  and  $\gamma\pi\pi$  current operators, and  $\tilde{J}_{IN}^\mu(q)$  is the reduced Kroll-Ruderman term [Fig. 1(d)]. We adopt a convention where the single particle currents,  $\tilde{j}_N^\mu$  and  $\tilde{j}_\pi^{ij\mu}$ , and the propagators include the overall factor of “ $i$ ” which multiplies all Feynman matrix elements (the Rule 0 of Ref. [40]), while the vertex functions do not (see Appendix A). The additional driving terms shown in diagrams (e) and (f) and the specific forms of the factors introduced in Eq. (2.16) will be given as they are needed in the following discussion.

The bare, reduced  $\pi NN$  vertex,  $\tilde{\Gamma}$ , is a superposition of pseudoscalar and pseudovector couplings

$$\tilde{\Gamma}_{N0}(k', P) = g \left( \lambda - \frac{1-\lambda}{2m} \not{k}' \right) \gamma_5, \quad (2.17)$$

where  $g$  is the  $\pi NN$  coupling constant and  $\lambda$  is the mixing parameter. Note that the vertex does not depend on  $P$ . The dressed vertex, which includes all of the  $\pi N$  contact interactions, satisfies

$$\begin{aligned} \tilde{\Gamma}_N(k', p) &= \tilde{\Gamma}_{N0}(k', p) - \int dk'' \tilde{M}_c^{1/2}(k', k'', p) \tilde{S}_N(p - k'') \tilde{\Gamma}_{N0}(k'', p) \\ &= \tilde{\Gamma}_{N0}(k', p) - \int dk'' \tilde{V}_c^{1/2}(k', k'', p) \tilde{S}_N(p - k'') \tilde{\Gamma}_N(k'', p), \end{aligned} \quad (2.18)$$

where  $\tilde{V}_c^{1/2}$  is the reduced  $\pi N$  contact interaction (in the isospin 1/2 channel), and  $\tilde{M}_c^{1/2}$  is the reduced iteration of these contact interactions to all orders (see Ref. [7]), and

$$\int dk'' = \int \frac{d^3 k''}{2\omega_{k''} (2\pi)^3}. \quad (2.19)$$

In the third term of Eq. (2.16), the vertex  $\tilde{\Gamma}_N(k' - q, p)$  describes the coupling of a nucleon to an *off-shell* pion, which is, strictly speaking, an amplitude outside of the framework of our model. However, since the reduced contact interactions  $\tilde{V}_c$  do not depend on the pion momenta (see the next section) and the reduced bare vertex depends on pion the momentum only through the  $(1-\lambda)\not{k}$  term in Eq. (2.17), the reduced off shell vertex is easily obtained by simply using the (correct) off-shell pion four-momentum in the formula for the on-shell vertex.

The full result for pion photoproduction, including final state interactions, will be written

$$M_{\pi\gamma}^i(k', q, P) = -ie \epsilon_\mu \mathcal{J}^{i\mu}(k', q, P) \quad (2.20)$$

where the current  $\mathcal{J}^\mu$  is a sum of the Born terms and integrals over the  $\pi N$  scattering amplitude [the diagrams shown in Fig. 2(a)–(f)]

$$\begin{aligned} \mathcal{J}^{i\mu}(k', q, P) &= \tilde{J}^{i\mu}(k', q, P) \\ &\quad - \int dk'' \tilde{M}_{\pi\pi}(k', k'', P) \tilde{S}_N(p'') \tilde{J}^{i\mu}(k'', q, P). \end{aligned} \quad (2.21)$$

Note that this equation is merely a statement of Eq. (2.3).

We are now ready to prove that the expression (2.21) is gauge invariant.

#### D. Gauge invariance

Using the notation and the relativistic equations discussed above, we will now show that the photoproduction amplitude obtained from the driving terms

shown in Fig. 1 is gauge invariant. As mentioned in the previous section, the  $\gamma NN^*$ ,  $\gamma N\Delta$ ,  $\gamma ND_{13}$ ,  $\rho\pi\gamma$ , and  $\omega\pi\gamma$  couplings are separately gauge invariant, so contributions to diagrams 1(a)–(c) from these resonances will be ignored here. The proof will follow the method introduced by Gross and Riska [35].

The *reduced* single nucleon current operator, denoted by  $\tilde{j}_N^\mu$  above, and the *reduced* single pion current operator, denoted by  $\tilde{j}_\pi^{ij\mu}$  above, have the following structure

$$\begin{aligned}\tilde{j}_N^\mu(p', p) &= \tau_p \tilde{j}_{N0}^\mu(p', p) \\ \tilde{j}_\pi^{ij\mu}(k', k) &= -i\epsilon_{ij3} \tilde{j}_{\pi 0}^\mu(k', k),\end{aligned}\quad (2.22)$$

where  $p$  and  $p'$  are the four momenta of the incoming and outgoing (off-shell) nucleon,  $\tau_p = \frac{1}{2}(1 + \tau_3)$  is charge operator for the nucleon (we ignore the nucleon anomalous magnetic moment term here because it is separately gauge invariant, but it is included in the full calculation), and  $k, j$  and  $k', i$  are the four momenta and isospin of the incoming and outgoing pion, respectively.

The proof begins with the fact that the current operators  $\tilde{j}_{N0}^\mu$  and  $\tilde{j}_{\pi 0}^\mu$ , can be constructed so as to satisfy Ward-Takahashi (WT) identities involving the *damped* propagators. These WT identities are (recall that the charge has been removed so that the current is normalized to  $j_{N0}^\mu \simeq \gamma^\mu$ )

$$q_\mu \tilde{j}_{N0}^\mu(p', p) = [\tilde{S}_N^{-1}(p) - \tilde{S}_N^{-1}(p')] \quad (2.23)$$

and

$$q_\mu \tilde{j}_{\pi 0}^\mu(k', k) = [\tilde{\Delta}_\pi^{-1}(k) - \tilde{\Delta}_\pi^{-1}(k')]. \quad (2.24)$$

The damped nucleon propagator  $\tilde{S}_N(p)$  and the damped pion propagator  $\tilde{\Delta}_\pi(k)$  are

$$\tilde{S}_N(p) = \frac{f_N^2(p^2)}{m - \not{p} - i\epsilon} = f_N^2(p^2) S_N(p^2) \quad (2.25)$$

and

$$\tilde{\Delta}_\pi(k) = \frac{f_\pi^2(k^2)}{\mu^2 - k^2 - i\epsilon} = f_\pi^2(k^2) \Delta(k^2), \quad (2.26)$$

where  $f_N(p^2)$  and  $f_\pi(k^2)$  are phenomenological form factors. The nucleon form factor,  $f_N(p^2)$ , has already been discussed; the pion form factor,  $f_\pi(k^2)$ , would occur only in diagrams 1(c), (e1) and (e2), and their final state interaction contributions, but we shall see later that it cancels and never enters into the final

result. Note that these form factors are unity when the particles are on their mass-shell:  $f_N(m^2) = 1 = f_\pi(\mu^2)$ .

Now compute the four-divergence of the nucleon pole contributions to the Born terms 1(a)–(d), given in Eq. (2.16) above. Allowing for the fact that the final nucleon will be off shell when the Born terms are used to calculate the final state interactions, and that the form factors are unity when the particle is on-shell, the Ward-Takahashi identities give

$$\begin{aligned}q_\mu \left( \tilde{j}^{i\mu} \right)_{a-d} &= \tau_i \tau_p \tilde{\Gamma}_{N0}(k', P) \tilde{S}_N(P) \left( 0 - \tilde{S}_N^{-1}(P) \right) \\ &\quad \tau_p \tau_i \left( \tilde{S}_N^{-1}(p - k') - \tilde{S}_N^{-1}(p') \right) \tilde{S}_N(p - k') \tilde{\Gamma}_N(k', p) \\ &\quad - i\epsilon_{ij3} \tau_j \left( \tilde{\Delta}^{-1}(k' - q) - 0 \right) \tilde{\Delta}(k' - q) \tilde{\Gamma}_N(k' - q, p) + q_\mu \tilde{J}_{IN}^{i\mu}(q) \\ &= -\tau_i \tau_p \tilde{\Gamma}_{N0}(k', P) + \tau_p \tau_i \tilde{\Gamma}_N(k', p) \\ &\quad - i\epsilon_{ij3} \tau_j \tilde{\Gamma}_N(k' - q, p) + q_\mu \tilde{J}_{IN}^{i\mu}(q) \\ &\quad - \tau_p \tau_i \tilde{S}_N^{-1}(p') \tilde{S}_N(p - k') \tilde{\Gamma}_N(k', p).\end{aligned}\quad (2.27)$$

Using the relativistic wave equation (2.18) for the dressed vertex permits us to write

$$\begin{aligned}q_\mu \left( \tilde{j}^{i\mu} \right)_{a-d} &= - \left[ \tau_i \tau_p \tilde{\Gamma}_{N0}(k', P) - \tau_p \tau_i \tilde{\Gamma}_{N0}(k', p) \right. \\ &\quad \left. + i\epsilon_{ij3} \tau_j \tilde{\Gamma}_{N0}(k' - q, p) - q_\mu \tilde{J}_{IN}^{i\mu}(q) \right] \\ &\quad - \tau_p \tau_i \int dk'' \tilde{V}_c^{1/2}(k', k'', p) \tilde{S}_N(p - k'') \tilde{\Gamma}_N(k'', p) \\ &\quad + i\epsilon_{ij3} \tau_j \int dk'' \tilde{V}_c^{1/2}(k' - q, k'', p) \tilde{S}_N(p - k'') \tilde{\Gamma}_N(k'', p) \\ &\quad - \tau_p \tau_i \tilde{S}_N^{-1}(p') \tilde{S}_N(p - k') \tilde{\Gamma}_N(k', p).\end{aligned}\quad (2.28)$$

Next, we recall that  $\tilde{\Gamma}_{N0}(k', P)$  does not depend on  $P$ , and observe that

$$\tilde{\Gamma}_{N0}(k' - q, p) = \tilde{\Gamma}_{N0}(k', p) + \frac{(1 - \lambda) \not{q}}{2m} g \gamma_5. \quad (2.29)$$

Hence, since  $\tau_i \tau_p - \tau_p \tau_i = -i\epsilon_{ij3} \tau_j$ , we see that the first four terms in square brackets in Eq. (2.28) will be zero provided

$$q_\mu \tilde{J}_{IN}^{i\mu}(q) = i\epsilon_{ij3} \tau_j \frac{(1 - \lambda) \not{q}}{2m} g \gamma_5. \quad (2.30)$$

This constraint will be satisfied by the Kroll-Ruderman term given in Sec. IV. Using this constraint, and the fact that the reduced  $\pi N$  contact interaction,  $\tilde{V}_c(k', k'', p) = \tilde{V}_c(p)$ , depends only on the *total* momentum  $p$ , the divergence of the diagrams in Fig. 1(a)–(d) becomes finally

$$q_\mu \left( \tilde{j}^{i\mu} \right)_{a-d} = -\tau_i \tau_p \int dk'' \tilde{V}_c^{1/2}(p) \tilde{S}_N(p - k'') \tilde{\Gamma}_N(k'', p) \\ - \tau_p \tau_i \tilde{S}_N^{-1}(p') \tilde{S}_N(p - k') \tilde{\Gamma}_N(k', p). \quad (2.31)$$

Now we add in the final state interactions from diagrams 2(a)–(d). It is convenient at this point to consider the final state interactions in the isospin  $I = 1/2$  and  $3/2$  states separately. These states can be separated out by the isospin  $1/2$  and  $3/2$  projection operators, which are

$$\mathcal{I}_{1/2}^{ij} = \frac{1}{3} \tau_i \tau_j \\ \mathcal{I}_{3/2}^{ij} = \delta_{ij} - \frac{1}{3} \tau_i \tau_j, \quad (2.32)$$

where  $i$  and  $j$  are the isospins of the outgoing and incoming pions, respectively. Hence the first term in Eq. (2.31) is pure  $I = 1/2$

$$\mathcal{I}_{3/2}^{ij} \tau_j = [\delta_{ij} - \frac{1}{3} \tau_i \tau_j] \tau_j = 0 \quad (2.33)$$

and does not contribute to the discussion of  $I = 3/2$  gauge invariance. The second term in Eq. (2.31) contributes to both isospin channels:

$$\mathcal{I}_{1/2}^{ij} \tau_p \tau_j = \frac{1}{2} \tau_i (1 - \frac{1}{3} \tau_3) \\ \mathcal{I}_{3/2}^{ij} \tau_p \tau_j = \mathcal{I}_{3/2}^{i3}, \quad (2.34)$$

but is zero for the Born terms because the final nucleon is on shell. Hence the full contribution of the  $I = 3/2$  final states to the photoproduction amplitude, Eq. (2.21), from the terms driven by the diagrams (a)–(d) is

$$q_\mu \left( \mathcal{J}_{3/2}^\mu \right)_{a-d} = \int dk'' \tilde{M}_{\pi\pi}^{3/2}(k', k'', P) \tilde{S}_N(P - k'') \tilde{S}_N^{-1}(P - k'') \\ \times \tilde{S}_N(p - k'') \tilde{\Gamma}_N(k'', p) \\ = \int dk'' \tilde{M}_{\pi\pi}^{3/2}(k', k'', P) \tilde{S}_N(p - k'') \tilde{\Gamma}_N(k'', p), \quad (2.35)$$

where the isospin factors can be dropped after Eq. (2.34) has been used. If the amplitude, as presently constructed, were gauge invariant, Eq. (2.35) would give zero. We must add several extra terms in order to get a gauge invariant result.

These extra terms are driven by the diagrams shown in Fig. 1(e1)–(e3). The pion loop in diagrams (e1) and (e2) contributes an isospin factor  $-i\epsilon_j \epsilon_3 \tau_\ell$ , where  $j$  is the isospin of the pion after its interaction with the photon. This factor can be decomposed into isospin  $1/2$  and  $3/2$  parts

$$-i\epsilon_j \epsilon_3 \tau_\ell = -\mathcal{I}_{3/2}^{j3} + 2\mathcal{I}_{1/2}^{j3}. \quad (2.36)$$

For diagram (e3), we need the isospin structure of the  $\gamma + \pi + N \rightarrow \Delta$  four point current, which will be shown in Sec. IVC to have the form

$$\tilde{j}_{I\Delta}^{j\nu\mu}(q, P) = -i\epsilon_j \epsilon_3 T_\ell^\dagger \tilde{j}_{I\Delta}^\mu(q, P), \quad (2.37)$$

where  $T_i$  is the isospin  $3/2 \rightarrow 1/2$  transition operator (and  $T^\dagger$  the  $1/2 \rightarrow 3/2$  transition operator) with the property

$$T_i T_j^\dagger = (\delta_{ij} - \frac{1}{3} \tau_i \tau_j) = \mathcal{I}_{3/2}^{ij}, \quad (2.38)$$

and  $\tilde{j}_{I\Delta}^\mu(q, P)$  is the reduced, isospin  $3/2$  interaction current, with  $q$  the momentum of the incoming photon,  $\mu$  its polarization index,  $P$  the momentum of the outgoing  $\Delta$ , and the four vector index of the outgoing  $\Delta$ ,  $\nu$ , suppressed. (Note that the definition and normalization of  $T$  used in this paper differs from that used in [7].) When the four point delta current is inserted into the pion loop in Fig. 1(e3), the isospin factor becomes

$$-i\epsilon_j \epsilon_3 T_\ell^\dagger \tau_j = T_\ell^\dagger \left( \mathcal{I}_{3/2}^{j3} - 2\mathcal{I}_{1/2}^{j3} \right) = T_3^\dagger \quad (2.39)$$

This factor of  $T_3^\dagger$  will eventually be combined with the transition operator  $T_i$  attached to the final  $\Delta \rightarrow \pi N$  vertex to give a factor of  $\mathcal{I}_{3/2}^{i3}$ , which is common to all of the three diagrams, and will be dropped. Hence the  $I = 3/2$  contribution from these diagrams is

$$\left( \mathcal{J}_{3/2}^\mu \right)_e = \int dk'' \left[ \tilde{V}_c^{3/2}(k', k'' + q, P) + \tilde{\Gamma}_{\Delta 0}(k', P) \tilde{G}_{\Delta 0}(P) \tilde{\Gamma}_{\Delta 0}(k'' + q, P) \right] \\ \times \tilde{\Delta}(k'' + q) \tilde{j}_{\pi 0}^\mu(k'' + q, k'') \tilde{S}_N(p - k'') \tilde{\Gamma}_N(k'', p) \\ - \int dk'' \tilde{\Gamma}_{\Delta 0}(k', P) \tilde{G}_{\Delta 0}(P) \tilde{j}_{I\Delta}^\mu(q, P) \tilde{S}_N(p - k'') \tilde{\Gamma}_N(k'', p), \quad (2.40)$$

where  $\tilde{\Gamma}_{\Delta 0}(k', P)$  is the *bare* but reduced (i.e. the nucleon *and* Delta form factors have been removed)  $\Delta \rightarrow N\pi$  vertex function and  $\tilde{G}_{\Delta 0}(P)$  is the damped (but undressed by the higher order  $\pi N$  interactions)  $\Delta$  propagator. All four vector

indices of the propagating Delta have been suppressed in Eq. (2.40), and all isospin operators have been removed, as discussed above. Using the WT identity to take the four-divergence of (2.40) gives

$$q_\mu \left( \tilde{J}_{3/2}^\mu \right)_e = - \int dk'' \left[ \tilde{V}_c^{3/2}(P) + \tilde{\Gamma}_{\Delta 0}(k', P) \tilde{G}_{\Delta 0}(P) \right. \\ \left. \times \left\{ \tilde{\Gamma}_{\Delta 0}(k'' + q, P) + q_\mu \tilde{J}_{I\Delta}^\mu(q, P) \right\} \right] \tilde{S}_N(p - k'') \tilde{\Gamma}_N(k'', p), \quad (2.41)$$

where we used the fact that  $\tilde{V}_c$  depends on  $P$  only. In Sec. IV we will show that the interaction current satisfies the following relation

$$q_\mu \tilde{J}_{I\Delta}^\mu(q, P) = -\tilde{\Gamma}_{\Delta 0}(k'' + q, P) + \tilde{\Gamma}_{\Delta 0}(k'', P). \quad (2.42)$$

Using this constraint, Eq. (2.41) becomes

$$q_\mu \left( \tilde{J}_{3/2}^\mu \right)_e = - \int dk'' \tilde{V}_{\pi\pi}^{3/2}(k', k'', P) \tilde{S}_N(p - k'') \tilde{\Gamma}_N(k'', p). \quad (2.43)$$

where

$$\tilde{V}_{\pi\pi}^{3/2}(k', k'', P) = \tilde{V}_c^{3/2}(k', k'', P) + \tilde{\Gamma}_{\Delta 0}(k', P) \tilde{G}_{\Delta 0}(P) \tilde{\Gamma}_{\Delta 0}(k'', P) \quad (2.44)$$

is the full kernel for  $\pi N$  scattering in the  $I = 3/2$  channel.

Including the final state interactions, the full contributions generated by diagrams 1(e) are

$$q_\mu \left( \mathcal{J}_{3/2}^\mu \right)_e = - \int dk'' \\ \left[ \tilde{V}_{\pi\pi}^{3/2}(k', k'', P) - \int dk \tilde{M}_{\pi\pi}^{3/2}(k', k, P) \tilde{S}_N(P - k) \tilde{V}_{\pi\pi}^{3/2}(k, k'', P) \right] \\ \times \tilde{S}_N(p - k'') \tilde{\Gamma}_N(k'', p) \\ = - \int dk'' \tilde{M}_{\pi\pi}^{3/2}(k', k'', P) \tilde{S}_N(p - k'') \tilde{\Gamma}_N(k'', p), \quad (2.45)$$

where, in the second step, we used the wave equation for  $\tilde{M}_{\pi\pi}$  to reduce the expression. Note that the contributions from diagrams (e), Eq. (2.45), cancel the contributions from diagrams (a)–(d), Eq. (2.35), proving that the  $I=3/2$  amplitude is gauge invariant.

We now turn to a discussion of the  $I = 1/2$  amplitude. The proof for this channel is similar to the one given above, but we must add the additional contributions from Eq. (2.31), and also be careful to consider the different isospin

operators which can contribute to this channel. Using the results from Eqs. (2.31), (2.34), (2.36), and generalizing the argument leading to (2.45), we get

$$q_\mu \left( \mathcal{J}_{1/2}^\mu \right)_{a-e} = -\tau_i \tau_p \int dk'' \tilde{V}_c^{1/2}(p) \tilde{S}_N(p - k'') \tilde{\Gamma}_N(k'', p) \\ + \tau_i \tau_p \int dk \tilde{M}_{\pi\pi}^{1/2}(k', k, P) \tilde{S}_N(P - k) \\ \times \int dk'' \tilde{V}_c^{1/2}(p) \tilde{S}_N(p - k'') \tilde{\Gamma}_N(k'', p) \\ + \frac{1}{2} \tau_i \left( 1 - \frac{1}{3} \tau_3 \right) \int dk'' \tilde{M}_{\pi\pi}^{1/2}(k', k'', P) \tilde{S}_N(p - k'') \tilde{\Gamma}_N(k'', p) \\ + \frac{2}{3} \tau_i \tau_3 \int dk'' \tilde{M}_{\pi\pi}^{1/2}(k', k'', P) \tilde{S}_N(p - k'') \tilde{\Gamma}_N(k'', p), \quad (2.46)$$

where the first term is the contribution of the Born terms from diagrams (a)–(d), the next two terms are the final state interactions generated by these Born terms, and the last term is the contribution from diagrams 1(e) and 2(e). To obtain the last term in the form given above, we followed steps similar to those leading to Eq. (2.45), eliminating the isospin 1/2 interaction currents associated with the diagrams 1(e3) and 2(e2) using a generalization of the constraint (2.42)

$$q_\mu \tilde{J}_{IB}^\mu(q, P) = -\tilde{\Gamma}_{B0}(k'' + q, P) + \tilde{\Gamma}_{B0}(k'', P), \quad (2.47)$$

where  $B = \{N, D_{13}\}$  (the Roper has no interaction current because, by construction, its coupling is independent of the pion momentum). In Sec. IV we will show that these constraints are satisfied.

Adding the last two terms in Eq. (2.46), and replacing  $\tilde{M}$  by its integral equation,  $\tilde{M} \rightarrow \tilde{V} - \int \tilde{M} \tilde{S} \tilde{V}$ , allows us to rewrite Eq. (2.46) in the following form:

$$q_\mu \left( \mathcal{J}_{1/2}^\mu \right)_{a-e} = -\tau_i \tau_p \int dk'' \left[ \tilde{V}_c^{1/2}(p) - \tilde{V}_{\pi\pi}^{1/2}(k', k'', P) \right] \tilde{S}_N(p - k'') \tilde{\Gamma}_N(k'', p) \\ + \tau_i \tau_p \int dk \tilde{M}_{\pi\pi}^{1/2}(k', k, P) \tilde{S}_N(P - k) \\ \times \int dk'' \left[ \tilde{V}_c^{1/2}(p) - \tilde{V}_{\pi\pi}^{1/2}(k, k'', P) \right] \tilde{S}_N(p - k'') \tilde{\Gamma}_N(k'', p). \quad (2.48)$$

Next, we recall from Eq. (2.44) that  $\tilde{V}_{\pi\pi}$  is the sum of a connected part and a resonance part. The contributions from the resonance part to Eq. (2.48) involves the following integrals

$$I_B = \int dk'' \bar{\Gamma}_{B0}(k'', P) \tilde{S}_N(p - k'') \tilde{\Gamma}_N(k'', p), \quad (2.49)$$

where  $B = \{N, N^*, D\}$ . However, for different reasons, these integrals (2.49) are all zero. The integral describing the  $N \rightarrow D_{13}$  transition is zero because the nucleon and  $D_{13}$  are orthogonal in our model, and the transition to the Roper is zero because the physical nucleon is defined by the condition that it be orthogonal to the Roper resonance at the nucleon pole (see the discussion in Ref. [7]). Finally, using the fact the  $\tilde{\Gamma}_{N0}(k'', P)$  does not depend on  $P$ , the  $N \rightarrow N$  contribution can be written

$$I_N = \int dk'' \bar{\Gamma}_{N0}(k'', p) \tilde{S}_N(p - k'') \tilde{\Gamma}_N(k'', p). \quad (2.50)$$

This is just is the value of the nucleon self energy at the nucleon pole, and, as discussed in Ref. [7], we adjust the parameters of the  $\pi N$  driving terms so as to insure that this quantity is zero. This constraint, which we call the *stability condition*, is an approximate way to include higher order interactions and ensures that the model is stable under small changes in the physical input. Because of these conditions, Eq. (2.48) reduces to

$$\begin{aligned} q_\mu \left( \mathcal{J}_{1/2}^{i\mu} \right)_{a-e} = & -\tau_i \tau_p \int dk'' \left[ \tilde{V}_c^{1/2}(p) - \tilde{V}_c^{1/2}(P) \right] \tilde{S}_N(p - k'') \tilde{\Gamma}_N(k'', p) \\ & + \tau_i \tau_p \int dk \tilde{M}_{\pi\pi}^{1/2}(k', k, P) \tilde{S}_N(P - k) \int dk'' \left[ \tilde{V}_c^{1/2}(p) - \tilde{V}_c^{1/2}(P) \right] \\ & \times \tilde{S}_N(p - k'') \tilde{\Gamma}_N(k'', p). \end{aligned} \quad (2.51)$$

This term is canceled by the second type of interaction current, illustrated in Figs. 1(f) and 2(f). This interaction current contributes the following terms to the amplitude

$$\begin{aligned} \left( \mathcal{J}_{1/2}^{i\mu} \right)_f = & -\tau_i \tau_p i \int dk'' \tilde{J}_{C1/2}^\mu(q, P) \tilde{S}_N(p - k'') \tilde{\Gamma}_N(k'', p) \\ & + \tau_i \tau_p i \int dk \tilde{M}_{\pi\pi}^{1/2}(k', k, P) \tilde{S}_N(P - k) \\ & \times \int dk'' \tilde{J}_{C1/2}^\mu(q, P) \tilde{S}_N(p - k'') \tilde{\Gamma}_N(k'', p), \end{aligned} \quad (2.52)$$

where the first term is the Born term shown in Fig. 1(f) and the second is the final state interaction shown in Fig. 2(f), and the current  $\tilde{J}_{C1/2}^\mu$  is defined as in Eq. (2.15). Later we will show that this term satisfies the following constraint

$$-i q_\mu \tilde{J}_{C1/2}^\mu(q, P) = \tilde{V}_c^{1/2}(P - q) - \tilde{V}_c^{1/2}(P), \quad (2.53)$$

which is precisely what is needed to cancel the contributions from Eq. (2.51). Hence, the gauge invariance of the  $I = 1/2$  channels has been proven.

We have proved that our theory involving the driving terms shown in Fig. 1 and the final state  $\pi N$  interactions shown in Fig. 2 is gauge invariant provided

- (i) the interaction currents satisfy the constraints (2.42), (2.47), and (2.53),
- (ii) the  $\gamma NN^*$ ,  $\gamma N\Delta$ ,  $\gamma ND_{13}$ ,  $\rho\pi\gamma$ , and  $\omega\pi\gamma$  couplings are all explicitly gauge invariant, and
- (iii) the reduced one body currents satisfy the WT identities (2.23) and (2.24).

These results will be demonstrated in the following sections.

We turn now to a detailed description of the modified  $\pi N$  scattering model.

### III. PION NUCLEON SCATTERING

In this section we describe the modifications to our  $\pi N$  scattering model previously published [7]. These modifications were made in order to: (i) improve the threshold behaviour (scattering lengths), (ii) more faithfully approximate the physics of the  $\pi\pi N$  channels which account for the inelasticity, (iii) reduce the complexity of the  $\pi\gamma$  interaction currents by minimizing the energy dependence of the  $\pi N$  interaction kernel which generates these interaction currents, (iv) remove the pole in the spin 3/2 propagator which occurs at  $P^2 = 0$ , and (v) introduce a form factor that eliminates all contributions from the space-like ( $P^2 < 0$ ) cut arising from the factor  $\sqrt{P^2}$ . While the  $P^2 < 0$  region is very far from the physical region ( $P^2 > (m + \mu)^2$ ) and plays no role in physical  $\pi N$  scattering, it does contribute when the  $\pi N$  nucleon interaction is imbedded in the  $\pi NN$  system, and we therefore decided to eliminate it now. Our discussion here will focus only on the changes being made in the original model; for a complete discussion the reader is referred to Ref. [7].

#### A. Relativistic contact terms

As in the original model, the relativistic contact terms come from the crossed nucleon pole (or nucleon exchange term), the effective  $\rho$  and  $\sigma$  type terms required by chiral symmetry, and an additional  $\rho$  exchange term unconstrained by chiral symmetry.

The *reduced* crossed nucleon pole diagram (expressed as a function of the pion momenta instead of the nucleon momenta, as was done in Ref. [7]) is

$$\tilde{V}_{c,N}(k', k, P) = Cg^2 \tau_i \tau_j f_N^2(u) \left( \frac{\lambda^2 - 1}{2m} + \left[ \frac{1}{m^2 - u} - \frac{(1 - \lambda)^2}{4m^2} \right] \mathcal{Q} \right) \quad (3.1)$$

where  $\mathcal{Q} = \frac{1}{2}(k' + k)$  and  $u = (P - k')^2$ . The simplest way to approximate the energy dependence implicit in  $\mathcal{Q}$  is to replace it by its value when all of the external particles are on mass-shell, which is

$$\mathcal{Q} = P - m. \quad (3.2)$$

We will use this approximation for the last term in Eq. (3.1), where  $\mathcal{Q}$  is multiplied by a constant, but this approximation, when used with the pole term  $1/(u - m^2)$ , gives a very inaccurate result when extrapolated to the nucleon pole at  $W = m$  [where, in the rest frame,  $P = (W, \mathbf{0})$ ]. In order to have a better extrapolation to  $W = m$ , which is very important for the calculation of the stability condition, and also to get the right threshold behavior, we approximate the pole term [the second term in Eq. (3.1)] as follows:

$$\frac{\mathcal{Q}}{m^2 - u} \simeq \frac{P}{\sqrt{P^2}(2m - \mu)} \quad (3.3)$$

This approximation is simpler than the one originally used in Ref. [7]. It is covariant, and the unwanted cut at space-like values of  $P^2$ , which can be reached when the  $\pi N$  amplitude is imbedded in  $NN$  scattering, can be eliminated by the nucleon form factor Eq. (1.11). With these approximations, the contact term generated by the crossed nucleon pole is

$$\tilde{V}_{c,N}(k', k, P) = Cg^2 \tau_i \tau_j f_0^2 \left( \frac{\lambda^2 - 1}{2m} + \frac{P}{\sqrt{P^2}(2m - \mu)} - \frac{(1 - \lambda)^2}{4m^2} (P - m) \right), \quad (3.4)$$

where  $f_0 = f[(m - \mu)^2]$  is the value of the nucleon form factor for the intermediate nucleon evaluated at the  $\pi N$  threshold.

Putting the pions on shell, the exact crossed pole diagram (3.1) and the approximate expression (3.4) can be compared below the physical  $\pi N$  threshold. In this region, the approximation (3.4) agrees well with the exact crossed diagram (3.1) when it is averaged over the pion three-momentum (such as would occur when  $V_c$  is used as a kernel); it gives only a 7% error when iterated once. The

approximation is also close to the exact crossed diagram above threshold; at  $W = 1550$  MeV it disagrees with the exact result by only 15%.

The crossed diagrams for the baryon resonances ( $N^*$ ,  $\Delta$ ,  $D_{13}$ ) are also approximated in the same way as the crossed nucleon diagram. In this approximation the  $\Delta$  and  $D_{13}$  crossed diagrams are zero, and the Roper crossed diagram becomes

$$\tilde{V}_{c,N^*}(k', k, P) = g_{N^*}^2 \tau_i \tau_j \left[ \frac{m^* - 2m + P}{m^{*2} - (m - \mu)^2} \right]. \quad (3.5)$$

With the approximation (3.2) for  $\mathcal{Q}$ , the  $\rho$  and  $\sigma$ -like contact terms are

$$\tilde{V}_{c,\sigma\rho}(k', k, P) = -C \frac{g^2}{m} f_0^2 \left[ \delta_{ij} \lambda^2 + [\tau_j, \tau_i] (1 - \lambda)^2 \frac{P - m}{4m} \right], \quad (3.6)$$

and the free  $\rho$  exchange term is

$$\tilde{V}_{c,\rho}^{\pi\pi}(k', k, P) = -C_\rho \frac{g^2}{4m^2} f_0^2 [\tau_j, \tau_i] (P - m), \quad (3.7)$$

where, as in Ref. [7], the constant  $C$  is fixed by the condition  $Cf_0^2 = f_N^2[(m + \mu)^2]$  and  $C_\rho$  is a free parameter related to the strength of the  $\rho$  exchange pole.

Note that all of these contact terms depend only on the *total* four-momentum  $P$ , and that the sum of these contributions has the simple form

$$\tilde{V}_c(P) = A + A_0 \frac{P}{\sqrt{P^2}} + BP, \quad (3.8)$$

where  $A$ ,  $A_0$  and  $B$  are constants. This result will be important in the construction of interaction currents in the next section.

## B. $\Delta$ and $D_{13}$ vertices

The Feynman rules for the reduced  $\pi N \Delta$  and  $\pi N D_{13}$  vertices used in our modified model are

$$T_j \tilde{\Gamma}_{\Delta 0}^\mu(k', P) = T_j \left( \frac{g_\Delta}{\mu} \right) k'_\nu \Theta^{\nu\mu}(P) \quad (3.9)$$

and

$$\tau_j \tilde{\Gamma}_{D_0}^\mu(k', P) = i\tau_j \left( \frac{g_D}{\mu} \right) k'_\nu \Theta^{\nu\mu}(P) \gamma_5, \quad (3.10)$$

where  $k'$  is the momentum of the outgoing pion (we use a different sign convention from that used in [7]),  $j$  is its isospin,  $P$  is the momentum of the incoming baryon,  $T_j^3$  is the isospin  $3/2 \rightarrow 1/2$  transition operator, and  $\Theta_{\mu\nu}(P)$  is the covariant spin  $3/2$  projection operator:

$$\Theta_{\mu\nu}(P) = -g_{\mu\nu} + \frac{1}{3}\gamma_\mu\gamma_\nu + \frac{1}{3}\left(\frac{P_\mu\gamma_\nu P_\nu + P_\nu\gamma_\mu P_\mu}{P^2}\right). \quad (3.11)$$

Note that the form factors of the nucleon and baryon have both been removed from (3.9) and (3.10) because these vertices are *reduced*, and that the  $\Gamma$ 's do not contain the isospin operators. As discussed above (Sec. IG) the pole at  $P^2 = 0$  which appears in  $\Theta_{\mu\nu}(P)$  is removed by the (new) form factors (contained in the baryon propagators connected to the baryon vertices) which are zero at  $P^2 = 0$ .

### C. Inelastic channels

The inelasticity in the  $P_{11}$  and  $D_{13}$  channels is due to the opening of the  $\pi\pi N$  channel. In our new model we assume that these two pions are bound together as a scalar particle  $\sigma^*$ . The mass of this particle is taken to be the same as the mass of two pions, 278 MeV. The reduced vertex for the  $N^* \rightarrow \sigma^* + N$  transition is

$$\tilde{\Gamma}'_{N^*}(k, P) = -i\left(g'_{1N^*} + g'_{2N^*}\frac{\not{k}}{2m}\right), \quad (3.12)$$

and for the  $D \rightarrow \sigma^* + N$  transition is

$$\tilde{\Gamma}'_D{}^\mu(k, P) = -\frac{1}{\mu}\left(g'_{1D} + g'_{2D}\frac{\not{k}}{2m}\right)k_\nu\Theta^{\nu\mu}(P), \quad (3.13)$$

where  $k$  and  $P$  are the momenta of the outgoing  $\sigma^*$  and the incoming baryon resonance, respectively. We were able to fit the data quite well without including the second term in the  $D_{13}$  and  $N^*$  coupling (i.e.  $g'_{2D} = g'_{2N^*} = 0$ ).

We now turn to a discussion of pion photoproduction.

## IV. PION PHOTOPRODUCTION

This last section is divided into four subsections. In the first we write down all of the couplings which describe the direct electromagnetic production of the

Roper,  $\Delta$ , and  $D_{13}$  from the nucleon. These expressions contain the precise definitions of the resonance photoproduction parameters given in Table II, and are individually gauge invariant, which justifies neglecting them in the discussion given in Section II. Next, we construct off-shell current operators for the single nucleon and single pion which are consistent with the WT identities Eqs. (2.23) and (2.24). These current operators are modified by the presence of the nucleon and pion form factors. In the third subsection we construct the interaction currents implied by the momentum dependence of the electromagnetic couplings and the contact interaction  $\tilde{V}_c$  [given in Eq. (3.8)]. To obtain these interaction currents, we use minimal substitution, and then demonstrate that they satisfy the necessary constraints obtained in Section II. Finally, we assemble the pieces and construct the actual pion-photoproduction driving terms which fully define the model.

### A. Electromagnetic couplings

In this subsection we define the electromagnetic transition currents for the baryon resonances,  $\gamma NB$ . We have removed an overall factor of  $e$  from each current.

#### 1. Delta current

According to Jones and Scadron [41] the  $\gamma N\Delta$  transition current can be written in terms of a standard "normal parity" set of invariants  $\mathcal{O}_i^{\nu\mu}\gamma_5$ . For real photons this gives

$$j_\Delta^{\nu\mu}(P, p) = -T_3[G_1\mathcal{O}_1^{\nu\mu} + G_2\mathcal{O}_2^{\nu\mu}]\gamma_5, \quad (4.1)$$

where  $T_3$  is the third component of the isospin  $1/2 \rightarrow 3/2$  transition operator, and the current conserving spin invariants are

$$\begin{aligned} \mathcal{O}_1^{\nu\mu} &= (\not{q}g^{\nu\mu} - q^\nu\gamma^\mu) \\ \mathcal{O}_2^{\nu\mu} &= (q^\nu P'^\mu - q.P'g^{\nu\mu}). \end{aligned} \quad (4.2)$$

Here  $q$  is the photon momentum,  $\mu$  is its polarization index,  $\nu$  is the polarization index of the outgoing  $\Delta$ , and  $P' = \frac{1}{2}(p + P)$ , where  $p$  and  $P$  are the four-momentum of nucleon and  $\Delta$ , respectively. The  $G_1$  and  $G_2$  couplings are often written in terms of the magnetic coupling  $G_M$  and the electric coupling  $G_E$ :

$$\begin{aligned}
G_M &= \frac{m}{3} \left[ (3M + m) \frac{G_1}{M} + (M - m)G_2 \right] \\
G_E &= \frac{m}{3} (M - m) \left[ \frac{G_1}{M} + G_2 \right], \quad (4.3)
\end{aligned}$$

where  $M$  is the  $\Delta$  mass.

Benmerrouche et.al. [39] obtain  $N\Delta$  transition currents from the following two contributions to the Lagrangian

$$\begin{aligned}
L_{\gamma N\Delta}^1 &= i \frac{eg_1}{2m} T_3 \bar{\Psi}_\nu \Sigma^{\nu\lambda}(Y) \gamma^\mu \gamma_5 \psi F_{\mu\lambda} + h.c. \\
L_{\gamma N\Delta}^2 &= -\frac{eg_2}{4m^2} T_3 \bar{\Psi}_\nu \Sigma^{\nu\lambda}(X) \gamma_5 \partial^\mu \psi F_{\lambda\mu} + h.c., \quad (4.4)
\end{aligned}$$

where  $\psi$  and  $\Psi_\mu$  are the nucleon and delta fields, respectively, and  $\Sigma_{\mu\nu}(X)$  is

$$\Sigma_{\mu\nu}(X) = g_{\mu\nu} + \left[ \frac{1}{2}(1 + 4X)A + X \right] \gamma_\mu \gamma_\nu, \quad (4.5)$$

where  $A$  and  $X$  are parameters. The interaction derived from Eq. (4.4) using the  $g_{\mu\nu}$  term in  $\Sigma_{\mu\nu}(X)$  (and removing the factor of  $e$ ) gives Eq. (4.1) with

$$\begin{aligned}
G_1 &= \frac{g_1}{2m} \\
G_2 &= \frac{g_2}{4m^2}. \quad (4.6)
\end{aligned}$$

The couplings of Refs. [39] and [41] therefore differ by an extra term which depends on  $X$ , and which can be shown to vanish at the  $\Delta$  pole.

In order to be consistent with our pion-nucleon model, we introduce a new  $\gamma N\Delta$  current which has almost the same form as the current derived from the Lagrangian (4.4). The full current,  $j_\Delta^{\nu\mu}(P, p)$  is related to a *reduced* current  $\tilde{j}_\Delta^{\nu\mu}(P, p)$  by

$$j_\Delta^{\nu\mu}(P, p) = f_N(p^2) f_\Delta(P^2) \tilde{j}_\Delta^{\nu\mu}(P, p), \quad (4.7)$$

where  $f_N$  and  $f_\Delta$  are the nucleon and  $\Delta$  form factors, and the reduced current is

$$\tilde{j}_\Delta^{\nu\mu}(P, p) = T_3 \frac{\Theta^\nu_\lambda(P)}{f_\Delta^2(P^2)} \left( \frac{P^2}{m_\Delta^2} \right)^2 \left[ \frac{g_{1\Delta}}{2m} \mathcal{O}_1^{\lambda\mu} + \frac{g_{2\Delta}}{4m^2} \mathcal{O}_2^{\lambda\mu} \right] \gamma_5. \quad (4.8)$$

Note that the reduced transition current (4.8) has been divided by the square of the  $\Delta$  form factor, cancelling the  $\Delta$  form factors contained in the damped  $\Delta$

propagator to which this current is connected. This cancellation is identical to one which occurs naturally in the pion Born term (as discussed in Sec. IVB2 below), and hence is consistent with the treatment of other electromagnetic currents. It also improved our ability to fit the  $E_{1+}$  and  $M_{1+}$  amplitudes. The  $(P^2/m_\Delta^2)^2$  factor in the reduced current is introduced to kill the pole in  $\Theta^\mu_\lambda(P)$  and to improve the fit. All of these factors can be incorporated without spoiling gauge invariance because the  $\gamma N\Delta$  transition current is separately gauge invariant.

Because of the properties of the spin 3/2 projection operator, our coupling (4.8), the coupling derived from Eq. (4.4), and the coupling (4.1) give the same scattering amplitude.

## 2. Roper current

The reduced  $\gamma NN^*$  transition current is

$$\tilde{j}_{N^*}^\mu(P, p) = \tau_p \frac{1}{f_{N^*}^2(P^2)} \left( g_{1N^*} \left[ \gamma^\mu - \frac{(P+p)^\mu \not{p}}{P^2 - p^2} \right] + g_{2N^*} \frac{i \sigma^{\mu\nu} q_\nu}{2m} \right), \quad (4.9)$$

where  $q, p$  and  $P$  are the momenta of the photon, the nucleon and the Roper, respectively, and  $g_{1N^*}$  and  $g_{2N^*}$  are the strength of the two independent couplings. We divide the Roper current by  $f_{N^*}^2$  in order to be consistent with the Delta. Note that

$$q_\mu \tilde{j}_{N^*}^\mu(P, p) = 0, \quad (4.10)$$

showing that all diagrams containing the Roper transition current are individually gauge invariant.

## 3. $D_{13}$ current

Like the  $\Delta$ , the  $D_{13}$  also has two independent couplings. The reduced  $D_{13}$  current is similar to the  $\Delta$  current except it has an opposite parity and isospin 1/2. The current is

$$\tilde{j}_D^{\nu\mu}(P, p) = -i \tau_3 \frac{\Theta^\nu_\lambda(P)}{f_D^2(P^2)} \left( \frac{P^2}{m_D^2} \right)^2 \left[ \frac{g_{1D}}{2m} \mathcal{O}_1^{\lambda\mu} + \frac{g_{2D}}{4m^2} \mathcal{O}_2^{\lambda\mu} \right]. \quad (4.11)$$



In order to be consistent with the treatment of the  $\Delta$  described above, we have also divided this current by the square of the form factor of the  $D_{13}$ , and multiplied by a factor of  $(P^2/m_D^2)^2$  to eliminate the pole in the spin 3/2 projection operator  $\Theta^\mu_\lambda(P)$ .

We now turn to a discussion of the construction of the off-shell current operators for the nucleon and the pion.

## B. Off-shell electromagnetic currents

As discussed in Sec. II, the reduced current operators must satisfy the WT identities Eqs. (2.23) and (2.24). These involve *damped* propagators, instead of bare propagators, and as a result the current operators will have a different structure from those usually encountered.

### 1. Nucleon current

A complete description of the general reduced off-shell nucleon current requires 12 invariant functions:

$$\begin{aligned} \tilde{j}_{N0}^\mu(p', p) = & F_1 \gamma^\mu + F_2 \frac{i \sigma^{\mu\nu} q_\nu}{2m} + F_3 q^\mu \\ & + \Lambda_-(p') \left[ F_4 \gamma^\mu + F_5 \frac{i \sigma^{\mu\nu} q_\nu}{2m} + F_6 q^\mu \right] \\ & + \left[ F_7 \gamma^\mu + F_8 \frac{i \sigma^{\mu\nu} q_\nu}{2m} + F_9 q^\mu \right] \Lambda_-(p) \\ & + \Lambda_-(p') \left[ F_{10} \gamma^\mu + F_{11} \frac{i \sigma^{\mu\nu} q_\nu}{2m} + F_{12} q^\mu \right] \Lambda_-(p), \end{aligned} \quad (4.12)$$

where the negative energy projection operator is

$$\Lambda_-(p) = \frac{m - \not{p}}{2m}. \quad (4.13)$$

This current operator must satisfy the Ward-Takahashi identity (2.23)

$$q_\mu \tilde{j}_{N0}^\mu(p', p) = \tilde{S}_N^{-1}(p) - \tilde{S}_N^{-1}(p') = \frac{m - \not{p}}{f_N^2(p^2)} - \frac{m - \not{p}'}{f_N^2(p'^2)}, \quad (4.14)$$

where  $f_N(p^2)$  is the nucleon form factor. Writing out both sides of this equation gives

$$\begin{aligned} & F_1 \not{q} + F_3 q^2 + \Lambda_-(p') [F_{10} \not{q} + F_{12} q^2] \Lambda_-(p) \\ & + \Lambda_-(p') [F_4 \not{q} + F_6 q^2] + [F_7 \not{q} + F_9 q^2] \Lambda_-(p) \\ & = \frac{2m}{f_N^2(p^2)} \Lambda_-(p) - \frac{2m}{f_N^2(p'^2)} \Lambda_-(p'). \end{aligned} \quad (4.15)$$

Equating the coefficients of the four independent Dirac matrices on each side of this equation gives four relations between the invariant functions which permits us to eliminate  $F_3$ ,  $F_6$ ,  $F_9$ , and  $F_{12}$

$$\begin{aligned} F_3 &= F_7 \left( \frac{m^2 - p^2}{2m q^2} \right) - F_4 \left( \frac{m^2 - p'^2}{2m q^2} \right) \\ F_{12} &= \frac{2m}{q^2} (F_7 - F_4) \\ F_6 &= -\frac{2m}{q^2 f'^2} + F_{10} \left( \frac{m^2 - p^2}{2m q^2} \right) + \frac{2m}{q^2} (F_1 + F_4) \\ F_9 &= \frac{2m}{q^2 f^2} - F_{10} \left( \frac{m^2 - p'^2}{2m q^2} \right) - \frac{2m}{q^2} (F_1 + F_7), \end{aligned} \quad (4.16)$$

where  $f = f_N(p^2)$  and  $f' = f_N(p'^2)$ . Substituting these constraints into Eq. (4.12) gives the following general result:

$$\begin{aligned} \tilde{j}_{N0}^\mu(p', p) = & F_0 \gamma^\mu + (F_1 - F_0) \tilde{\gamma}^\mu + F_2 \frac{i \sigma^{\mu\nu} q_\nu}{2m} \\ & + \Lambda_-(p') \left[ F_4 \tilde{\gamma}^\mu + F_5 \frac{i \sigma^{\mu\nu} q_\nu}{2m} \right] + \left[ F_7 \tilde{\gamma}^\mu + F_8 \frac{i \sigma^{\mu\nu} q_\nu}{2m} \right] \Lambda_-(p) \\ & + \Lambda_-(p') \left[ G_0 \gamma^\mu + (F_{10} - G_0) \tilde{\gamma}^\mu + F_{11} \frac{i \sigma^{\mu\nu} q_\nu}{2m} \right] \Lambda_-(p), \end{aligned} \quad (4.17)$$

where  $\tilde{\gamma}^\mu = \gamma^\mu - q^\mu \not{q}/q^2$ ,

$$\begin{aligned} F_0 &= \frac{1}{f'^2} \frac{m^2 - p'^2}{p^2 - p'^2} + \frac{1}{f^2} \frac{m^2 - p^2}{p'^2 - p^2} \\ G_0 &= \left( \frac{1}{f'^2} - \frac{1}{f^2} \right) \frac{4m^2}{p'^2 - p^2}, \end{aligned} \quad (4.18)$$

and, to eliminate kinematic singularities, we require that  $F_1 - F_0 = F_{10} - G_0 = F_4 = F_7 = 0$  at the photon point  $q^2 = 0$ . Hence, for real photons the terms

proportional to  $\tilde{\gamma}^\mu$  vanish, and we obtain the most general form for the current operator of a real photon:

$$\begin{aligned}\tilde{j}_{N0}^\mu(p', p) &= F_0 \gamma^\mu + F_2 \frac{i \sigma^{\mu\nu} q_\nu}{2m} \\ &+ \Lambda_-(p') F_5 \frac{i \sigma^{\mu\nu} q_\nu}{2m} + F_8 \frac{i \sigma^{\mu\nu} q_\nu}{2m} \Lambda_-(p) \\ &+ \Lambda_-(p') \left[ G_0 + F_{11} \frac{i \sigma^{\mu\nu} q_\nu}{2m} \right] \Lambda_-(p).\end{aligned}\quad (4.19)$$

For simplicity, in this calculation we take  $F_5 = F_8 = 0$  and  $F_2 = F_0 \kappa_N$ ,  $F_{11} = G_0 \kappa_N$ , where  $\kappa_N$  is the magnetic moment of the nucleon. If the initial nucleon is on-shell this gives

$$\tilde{j}_{N0}^\mu(p', p) = \frac{1}{f_N^2(p'^2)} \left( \gamma^\mu + \kappa_N \frac{i \sigma^{\mu\nu} q_\nu}{2m} \right). \quad (4.20)$$

Note the presence of the factor of  $1/f_N^2(p'^2)$ , which supports our decision to divide by the resonance form factor in the definitions of the transition currents (4.8), (4.9), and (4.11).

## 2. Pion current

Following Gross and Riska [35], a simple off-shell current operator which satisfies the WT identity (2.24) is

$$\tilde{j}_{\pi 0}^\mu(k', k) = (k + k')^\mu \left[ 1 + \frac{\Pi(k'^2) - \Pi(k^2)}{k'^2 - k^2} \right], \quad (4.21)$$

where  $k$  and  $k'$  are the momenta of the incoming and outgoing pion, and

$$\Pi(k^2) = \left[ \frac{1}{f_\pi^2(k^2)} - 1 \right] (k^2 - \mu^2) \quad (4.22)$$

and  $f_\pi(k^2)$  is the pion form factor. If the outgoing pion is on-shell, as occurs in the Born diagram Fig. 1c, the reduced current reduces to

$$\tilde{j}_{\pi 0}^\mu(k', k) = \frac{1}{f_\pi^2(k^2)} (k + k')^\mu. \quad (4.23)$$

When this current is used in the Born diagram Fig. 1c, the factor of  $1/f_\pi^2(k^2)$  is cancelled by the pion form factors in the damped pion propagator, Eq. (2.26).

## C. Interaction currents

In this subsection we derive the exact forms of the interaction currents introduced in Sec. II and shown in Figs. 1(d),(e3) and (f), and 2(e2) and (f).

### 1. The five-point current

We begin with a discussion of the five-point current,  $\tilde{J}_{C1/2}^\mu(q, P)$ , shown in Fig. 1(f). The discussion of gauge invariance in Sec. II showed us that the origin of this current is the dependence of the  $\pi N$  contact interaction, Eq. (3.8), on the total pion-nucleon momentum  $P$  in the channel which couples to the proton, where the isospin is  $1/2$  and the charge is  $e$ . Hence, to obtain this current we need only consider the effect of the replacement of the four-momentum  $P$  by  $P - e A$  (minimal substitution) in the  $I = 1/2$  part of the contact interaction (3.8). Such a replacement generates an electromagnetic interaction of the form

$$-ie \tilde{J}_{C1/2}^\mu(q, P) A_\mu = -e B^{1/2} \gamma^\mu A_\mu, \quad (4.24)$$

and hence the current is simply

$$-i \tilde{J}_{C1/2}^\mu(q, P) = -B^{1/2} \gamma^\mu. \quad (4.25)$$

Note that this current satisfies the constraint

$$\begin{aligned}-i q_\mu \tilde{J}_{C1/2}^\mu(q, P) &= -B^{1/2} \not{q} = -B^{1/2} [P - (P - \not{q})] \\ &= \tilde{V}_c^{1/2}(P - q) - \tilde{V}_c^{1/2}(P).\end{aligned}\quad (4.26)$$

In this case the interaction was linearly dependent on momentum and the interaction current was easily obtained directly. In the general case of an interaction with a non-linear momentum dependence the interaction current can be obtained following procedures suggested by Ohta [32], and worked out for several illustrative cases in Ref. [42].

### 2. The four-point currents

The four-point currents,  $\tilde{J}_{FB}^\mu(q, P)$  shown in Figs. 1(d) and 1(e3), appear because of the dependence of the  $\pi NN$ ,  $\pi N\Delta$  and  $\pi ND_{13}$  vertices on the momentum of the pion. The  $\pi NN^*$  vertex does not depend on the pion momentum

and therefore does not contribute a four-point current. These currents can all be obtained by minimal substitution.

We begin the discussion with the  $\pi NN$  vertex, which produces the familiar Kroll-Ruderman interaction current term. The reduced  $\pi NN$  vertex was given in Eq. (2.17). Minimal substitution requires that we replace the pion momentum,  $k'$ , by  $k' - \eta e A$ , where  $\eta = \pm 1$ , or 0, depending on the charge of the pion. Recalling that the operator for an outgoing  $\pi^\pm$  is  $\tau_\mp$ , the factor of  $-\eta e$  becomes

$$\begin{aligned}\tau_x &= \frac{1}{2}(\tau_+ + \tau_-) \rightarrow \frac{1}{2}(e\tau_+ - e\tau_-) = ie\tau_y \\ \tau_y &= -\frac{1}{2}i(\tau_+ - \tau_-) \rightarrow -\frac{1}{2}i(e\tau_+ + e\tau_-) = -ie\tau_x \\ \tau_z &\rightarrow 0.\end{aligned}\quad (4.27)$$

This substitution is summarized by  $\tau_i \rightarrow ie\epsilon_{ij3}\tau_j$ , giving

$$\tilde{J}_{IN}^{i\mu}(q) = ie\epsilon_{ij3}\tau_j \frac{(1-\lambda)\gamma^\mu}{2m} g\gamma_5 \quad (4.28)$$

Note that the complete Kroll-Ruderman interaction current includes two terms. The first term, obtained above from minimal substitution, satisfies the inhomogenous constraint (2.30), while the second term, not obtainable from minimal substitution, satisfies  $q_\mu \tilde{J}_{IN}^{i\mu}(q) = 0$ . The full Kroll-Ruderman current is given in Eq. (4.37) below.

Next, consider the *conjugate* of the reduced  $\pi N\Delta$  vertex given in Eq. (3.9). This vertex depends on both the incoming pion momentum,  $k$  [and hence has the opposite sign from (3.9)], and the Delta momentum,  $P$ , but the dependence on the Delta momentum generates no interaction current in the rest frame of the Delta, and hence, because of covariance, vanishes in all frames. The  $k$  dependence generates a substitution similar to that given in Eq. (4.27), with all  $\tau_i$  replaced by  $-T_i^\dagger$ . Hence, according our conventions, the  $\gamma\pi N \rightarrow \Delta$  four-point current is

$$-ie\tilde{J}_{I\Delta}^{i\nu\mu} = i\left(ie\epsilon_{ij3}T_j^\dagger\right)\left(\frac{g\Delta}{\mu}\right)\Theta^{\nu\mu}(P) = -ie\left(-ie\epsilon_{ij3}T_j^\dagger\right)\tilde{J}_{I\Delta}^\mu, \quad (4.29)$$

where  $\tilde{J}_{I\Delta}^\mu$  was introduced in Sec. II, Eq. (2.37). Hence

$$\tilde{J}_{I\Delta}^\mu = \left(\frac{g\Delta}{\mu}\right)\Theta^{\nu\mu}(P), \quad (4.30)$$

and satisfies the constraint Eq. (2.42)

$$\begin{aligned}q_\mu \tilde{J}_{I\Delta 0}^{\nu\mu}(q, P) &= \left(\frac{g\Delta}{\mu}\right) q_\mu \Theta^{\nu\mu}(P) \\ &= \left(\frac{g\Delta}{\mu}\right) [\Theta^{\nu\mu}(P)(k+q)_\mu - \Theta^{\nu\mu}(P)k_\mu] \\ &= \bar{\Gamma}_{\Delta 0}(k, P) - \bar{\Gamma}_{\Delta 0}(k+q, P),\end{aligned}\quad (4.31)$$

as required for the proof of gauge invariance.

The four-point current generated from the  $\pi ND_{13}$  vertex can be obtained by the same manner. For the  $D_{13}$  current we have,

$$-ie\tilde{J}_{ID}^{\nu\mu} = -(ie\epsilon_{ij3}\tau_j)\left(\frac{gD}{\mu}\right)\gamma_5\Theta^{\nu\mu}(P) = -ie(-ie\epsilon_{ij3}\tau_j)\tilde{J}_{ID}^\mu. \quad (4.32)$$

Hence the  $D_{13}$  four point current

$$\tilde{J}_{ID}^\mu = i\left(\frac{gD}{\mu}\right)\gamma_5\Theta^{\nu\mu}(P), \quad (4.33)$$

satisfies the constraint Eq. (2.47), as required for gauge invariance.

## D. Driving terms

Using the electromagnetic currents described in the previous sections, this subsection gives explicit expressions for all of the driving terms shown in Fig. 1. For convenience, the direct and crossed nucleon pole contributions [Figs. 1(a) and (b)], the Kroll-Ruderman term [Fig. 1(d)], the nucleon pole contribution to Fig. 1(e3), and the five pion current [Fig. 1(f)] will be referred to as “nucleon” contributions. The meson exchange diagrams [Fig. 1(c)] and *all* of the loop contributions from off-shell pions [Figs. 1(e1) and (e2)] will be referred to as “meson” contributions. The resonance contributions to Figs. 1(a), (b), and (e3) will be discussed separately.

### 1. Nucleon

The direct nucleon pole diagram [Fig. 1(a)] is:

$$\left(\tilde{J}_N^{i\mu}\right)_a(k', q, P) = g\tau_i \left[\lambda - \frac{(1-\lambda)k'}{2m}\right] \gamma_5 \left(\frac{1}{m-P}\right) (\gamma^\mu \tau_p - \frac{1}{4m}[\gamma^\mu \not{P} - \not{P} \gamma^\mu] \kappa_N) \quad (4.34)$$

where  $\mu$  is the photon polarization vector index,  $q$  and  $k'$  are the photon and pion momenta respectively,  $i$  is the isospin of the outgoing pion, and  $\kappa_N = \frac{1}{2}[\kappa_p + \kappa_n + (\kappa_p - \kappa_n)\tau_3]$  is the nucleon anomalous magnetic moment.

Note that the  $\pi NN$  form factor does not appear in the direct pole diagram (4.34), because when one of the nucleons in the  $\gamma NN$  vertex is on-shell, the reduced current becomes Eq. (4.20), and the factor of  $1/f_N^2(P^2)$  in this equation cancels the form factors contained in the damped nucleon propagator, Eq. (2.25). Note also that the conjugate of the driving term (4.34) satisfies the relation

$$\begin{aligned} (\bar{J}_N^{i\mu})_a(k', q, P) &= \gamma_0 g(\gamma^{\mu\dagger} \tau_p - \frac{1}{4m}[\not{d}^\dagger \gamma^{\mu\dagger} - \gamma^{\mu\dagger} \not{d}^\dagger] \kappa_N) \\ &\quad \times \left( \frac{1}{m - P^\dagger} \right) \gamma_5 \left[ \lambda - \frac{(1-\lambda)\not{k}'^\dagger}{2m} \right] \tau_i \gamma_0 \\ &= -g(\gamma^\mu \tau_p - \frac{1}{4m}[\not{d} \gamma^\mu - \gamma^\mu \not{d}] \kappa_N) \left( \frac{1}{m - P} \right) \gamma_5 \left[ \lambda - \frac{(1-\lambda)\not{k}'}{2m} \right] \tau_i \\ &= -g(\gamma^\mu \tau_p + \frac{1}{4m}[\gamma^\mu \not{d} - \not{d} \gamma^\mu] \kappa_N) \left( \frac{1}{m - P} \right) \left[ \lambda + \frac{(1-\lambda)\not{k}'}{2m} \right] \gamma_5 \tau_i \\ &= -(\bar{J}_N^{i\mu})_a(q, k', P). \end{aligned} \quad (4.35)$$

Recalling the connection (2.15) between the current and the kernel, this relation leads to Eq. (2.9), the condition needed to give the correct unitarity relation.

Since the final nucleon can be off-shell, the crossed nucleon pole diagram [Fig. 1(b)] is

$$\begin{aligned} (\bar{J}_N^{i\mu})_b(k', q, P) &= [F_0 \bar{J}_N^\mu(p', Q) + G_0 \Lambda_-(p') \bar{J}_N^\mu(p', Q) \Lambda_-(Q)] \\ &\quad \times \left( \frac{f_N^2(Q^2)}{m - Q} \right) \bar{\Gamma}_N(k', p) \tau_i \end{aligned} \quad (4.36)$$

where  $\bar{J}_N^\mu(p', Q) = \gamma^\mu \tau_p - \frac{1}{4m}(\gamma^\mu \not{d} - \not{d} \gamma^\mu) \kappa_N$  is the full reduced nucleon current,  $F_0$  and  $G_0$  are functions of  $p'^2$  and  $Q^2$  defined in Eqs. (4.18) and (4.19),  $\bar{\Gamma}_N(k', p)$  is the reduced, dressed  $\pi NN$  vertex function, which satisfies Eq. (2.18),  $Q = p' - q = p - k'$  is the four-momentum of the virtual intermediate nucleon, and  $P = p + q = p' + k'$  is the total momentum. In this term the  $\pi NN$  form factor is not cancelled, because both nucleons in the  $\gamma NN$  vertex are off-shell.

As discussed above, the Kroll-Ruderman term, Fig. 1(d), has two parts. The first part, given in Eq. (4.28), is obtained from the momentum dependence of the  $\pi NN$  coupling using minimal substitution, and the second part is needed to insure that the low energy theorem [24] is independent of the mixing parameter  $\lambda$ . The complete Kroll-Ruderman term is therefore

$$(\bar{J}_N^{i\mu})_d = g \left[ i \epsilon_{ij3} \tau_j \frac{(1-\lambda)\gamma^\mu}{2m} + \frac{\lambda}{8m} [\gamma^\mu \not{d} - \not{d} \gamma^\mu] (\kappa_N \tau_j + \tau_j \kappa_N) \right] \gamma_5. \quad (4.37)$$

Note that the second term is separately gauge invariant, and therefore did not enter into the proof of gauge invariance presented in Sec. II.

The additional interaction current driving terms are obtained from the interaction currents worked out above. The nucleon contribution to the diagram shown in Fig. 1(e3) is obtained from Eq. (4.28)

$$\begin{aligned} (\bar{J}_N^{i\mu})_{e3}(k', q, P) &= -\tau_i \tau_3 \frac{g}{m} \bar{\Gamma}_{N0}(p', P) \bar{S}_N(P) (1-\lambda) \gamma^\mu \gamma_5 \\ &\quad \times \int \frac{d^3 k''}{(2\pi)^3 2\omega_{k''}} \frac{f_N^2[(p-k'')^2]}{(m - \not{p} + \not{k}'')} \bar{\Gamma}_N(k'', p). \end{aligned} \quad (4.38)$$

The contribution from the five-point contact current shown in Fig. 1(f) is obtained directly from the five-point current, Eq. (4.25),

$$(\bar{J}_N^{i\mu})_{f, \frac{1}{2}}(q, P) = -\tau_i \tau_p B^{1/2} \gamma^\mu \int \frac{d^3 k''}{(2\pi)^3 2\omega_{k''}} \frac{f_N^2[(p-k'')^2]}{(m - \not{p} + \not{k}'')} \bar{\Gamma}_N(k'', p). \quad (4.39)$$

Note that this current contributes only to the isospin 1/2 channel.

## 2. Mesons

The pion pole contribution to the meson exchange diagram, Fig. 1(c), is

$$(\bar{J}_\pi^{i\mu})_c(k', q, P) = -i \epsilon_{ij3} \tau_j \frac{(k' + k)^\mu}{\mu^2 - k^2} \bar{\Gamma}_N(k, p), \quad (4.40)$$

where  $k = p - p' = k' - q$  is the four-momentum of the off-shell pion. The vertex function  $\bar{\Gamma}_N(k, p)$  describes the coupling to an *off-shell* pion, which, because pions are on-shell in our propagators, does not appear as an elementary amplitude in our model. However, as discussed in Sec. II, the simple structure of the model permits us to obtain the reduced off-shell vertex function from the reduced on-shell one by simply using the correct off-shell pion four-momentum. Furthermore, the square of any pion form factor which might be associated with the damped propagator of the pion would be cancelled by the factor of  $1/f_\pi^2(k^2)$  in the off shell current [recall Eq. (4.23)], so no such form factor appears in the pion exchange diagram (4.40).

Contributions from off-shell pions also appear in the diagrams shown in Figs. 1(e1), and (e2). Together, these diagrams contribute

$$\begin{aligned} (\tilde{J}^{i\mu})_{e_1+e_2}(k', q, P) &= i\epsilon_{j\ell 3} \int \frac{d^3 k''}{(2\pi)^3 2\omega_{k''}} \tilde{V}_{\pi\pi}^{ij}(k', k''+q, P) \tau_\ell \frac{(2k''+q)^\mu}{\mu^2 - (k''+q)^2} \\ &\times \frac{f_N^2 [(p-k'')^2]}{m - \not{p} + \not{k}''} \tilde{\Gamma}_N(k'', p), \end{aligned} \quad (4.41)$$

where  $\tilde{V}_{\pi\pi}^{ij}(k', k''+q, P)$  is the reduced  $\pi N$  driving term, including *all* resonance contributions, for scattering of an incoming pion with isospin  $j$  to an outgoing pion with isospin  $i$ . Again, just as in the pion pole term (4.40), the pion form factor will cancel, showing that no pion form factor appears anywhere in the final result.

The meson driving terms also include additional contributions to Fig. 1(c) coming from  $\omega$  and  $\rho$  exchange. The  $\omega$  exchange diagram is

$$\begin{aligned} (\tilde{J}_\omega^{i\mu})_c(k', q, P) &= i\delta_{i3} \frac{f_{\omega NN} g_{\omega\pi\gamma}}{\mu [m_\omega^2 - (k'-q)^2]} \epsilon^{\mu\nu\lambda\rho} q_\nu k'_\lambda \left[ \gamma_\rho + \frac{\kappa_\omega}{2m} i\sigma_{\rho\eta} (k'-q)^\eta \right] \\ &= i\delta_{i3} \frac{f_{\omega NN} g_{\omega\pi\gamma}}{\mu} \left( 1 + \frac{\kappa_\omega}{2m} (\not{k}' - \not{q}) \right) \frac{q_\nu k'_\lambda \epsilon^{\mu\nu\lambda\rho} \gamma_\rho}{m_\omega^2 - (k'-q)^2}, \end{aligned} \quad (4.42)$$

where  $\epsilon_{0123} = 1$ . Using the identity

$$\epsilon^{\mu\nu\lambda\rho} \gamma_\rho = \frac{i\gamma_5}{6} [\gamma^\mu \gamma^\nu \gamma^\lambda + \gamma^\nu \gamma^\lambda \gamma^\mu + \gamma^\lambda \gamma^\mu \gamma^\nu - \gamma^\lambda \gamma^\nu \gamma^\mu - \gamma^\nu \gamma^\mu \gamma^\lambda - \gamma^\mu \gamma^\lambda \gamma^\nu] \quad (4.43)$$

the  $\omega$  exchange diagram reduces to

$$(\tilde{J}_\omega^{i\mu})_c(k', q, P) = \delta_{i3} \frac{f_{\omega NN} g_{\omega\pi\gamma}}{\mu} \left( 1 + \frac{\kappa_\omega}{2m} (\not{k}' - \not{q}) \right) \gamma_5 \frac{\not{k}' \not{q} \gamma^\mu - k \cdot q \gamma^\mu + k'^\mu \not{q}}{m_\omega^2 - (k-q)^2}, \quad (4.44)$$

where  $\not{q} \not{q} = q^2 = 0$ , and because the current is transverse,  $\gamma^\mu \not{q} = -\not{q} \gamma^\mu$ .

The  $\rho$  exchange diagram has the same structure as the  $\omega$  exchange diagram, except the  $\rho$  is isovector. Hence

$$(\tilde{J}_\rho^{i\mu})_c(k', q, P) = \tau_3 \frac{f_{\rho NN} g_{\rho\pi\gamma}}{\mu} \left( 1 + \frac{\kappa_\rho}{2m} (\not{k}' - \not{q}) \right) \gamma_5 \frac{\not{k}' \not{q} \gamma^\mu - k \cdot q \gamma^\mu + k'^\mu \not{q}}{m_\rho^2 - (k-q)^2}, \quad (4.45)$$

### 3. Roper

The Roper has the same spin-isospin structure as a nucleon, and therefore the direct and crossed Roper pole diagrams have the same structure as the nucleon pole diagrams. They are constructed from the  $\gamma NN^*$  transition current, Eq. (4.9). The direct Roper pole diagram [Fig. 1(a)] is

$$(\tilde{J}_{N^*}^{i\mu})_a(k', q, P) = g_{N^*} \tau_i \gamma_5 \left( \frac{1}{m^* - P} \right) \left( g_{1N^*} \tilde{\gamma}^\mu(P) - \frac{g_{2N^*}}{4m} [\gamma^\mu \not{q} - \not{q} \gamma^\mu] \right) \tau_p, \quad (4.46)$$

where

$$\tilde{\gamma}^\mu(P) = \gamma^\mu - \frac{P^\mu \not{q}}{P \cdot q}. \quad (4.47)$$

Letting  $Q = P - k' - q = p - k'$ , the crossed pole diagram [Fig. 1(b)] is

$$(\tilde{J}_{N^*}^{i\mu})_b(k', q, P) = g_{N^*} \tau_p \tau_i \left( g_{1N^*} \tilde{\gamma}^\mu(Q) - \frac{g_{2N^*}}{4m} [\gamma^\mu \not{q} - \not{q} \gamma^\mu] \right) \frac{1}{m^* - Q} \gamma_5 \quad (4.48)$$

Note that the  $N^*$  form factor in the current (4.9) is cancelled by the form factors in the damped  $N^*$  propagator, as we have seen in several previous cases.

### 4. Delta

In parallel with the approximations made in the  $\pi N$  calculation, the crossed  $\Delta$  pole contribution to Fig. 1(b) is taken to be zero. This approximation almost decouples the spin 3/2 channel from the spin 1/2 channel, allowing us to fit these different channels independently.

The direct  $\Delta$  pole contribution to Fig. 1(a) is obtained from the  $\gamma N \Delta$  transition current, Eq. (4.8),

$$(\tilde{J}_\Delta^{i\mu})_a(k', q, P) = T_i T_3 \left( \frac{g_\Delta}{\mu} \right) k'_\nu \Theta_{\nu\lambda}(P) \frac{(P^2/m_\Delta^2)^2}{m_\Delta - P} \left[ \frac{g_{1\Delta}}{2m} \mathcal{O}_1^{\lambda\mu} + \frac{g_{2\Delta}}{4m^2} \mathcal{O}_2^{\lambda\mu} \right] \gamma_5, \quad (4.49)$$

where  $\Theta_{\nu\lambda}$  is the spin 3/2 projection operator, and (4.49) has been simplified by using  $\Theta_{\nu\lambda} \Theta^{\lambda\mu} = -\Theta_{\nu\mu}$ . Note that the  $\Delta$  form factor in the current cancels a

similar form factor in the damped  $\Delta$  propagator, as we have seen several times before.

The Delta contribution to the four-point function in Fig. 1(e3) is constructed from the  $\gamma\pi N \rightarrow \Delta$  four-point current (4.29):

$$\begin{aligned} \left(\tilde{J}_\Delta^{i\mu}\right)_{e3}(k', q, P) &= -i \epsilon_{j\ell 3} T_i^\dagger T_j^\dagger \tau_\ell \left(\frac{g_\Delta}{\mu}\right)^2 \frac{f_\Delta^2(P^2)}{m_\Delta - P} k'_\lambda \Theta^{\lambda\mu}(P) \\ &\times \int \frac{d^3 k''}{(2\pi)^3 2\omega_{k''}} \frac{f_N^2(p - k'')}{(m - \not{p} + \not{k}'')} \tilde{\Gamma}_N(k'', p). \end{aligned} \quad (4.50)$$

Recalling that the isospin transition operators satisfy Eq. (2.38), and using Eq. (2.36), the isospin factor in (4.50) reduces to

$$-i \epsilon_{j\ell 3} T_i^\dagger T_j^\dagger \tau_\ell = -i T_{3/2}^{ij} \epsilon_{j\ell 3} \tau_\ell = -T_{3/2}^{ij} [T_{3/2}^{j3} - 2T_{1/2}^{j3}] = -T_{3/2}^{i3}. \quad (4.51)$$

### 5. $D_{13}$

The  $D_{13}$  resonance contributions to the diagrams 1(a) and (e3) are almost identical to those for the  $\Delta$ , except for a different isospin factor and some sign changes due to the opposite parity of the  $D_{13}$ .

The direct  $D_{13}$  pole contribution [Fig. 1(a)] is

$$\begin{aligned} \left(\tilde{J}_D^{i\mu}\right)_a(k', q, P) &= -\tau_i \tau_3 \left(\frac{g_D}{\mu}\right) k'_\nu \Theta^{\nu\lambda}(P) \frac{(P^2/m_D^2)^2}{m_D + P} \left[\frac{g_{1D}}{2m} \mathcal{O}_1^{\lambda\mu} - \frac{g_{2D}}{4m^2} \mathcal{O}_2^{\lambda\mu}\right] \gamma_5. \end{aligned} \quad (4.52)$$

The  $D_{13}$  contribution to the four-point current [Fig. 1(e3)] is:

$$\begin{aligned} \left(\tilde{J}_D^{i\mu}\right)_{e3}(k', q, P) &= -2\tau_i \tau_3 \left(\frac{g_D}{\mu}\right)^2 \frac{f_D^2(P^2)}{m_D + P} k'_\lambda \Theta^{\lambda\mu}(P) \\ &\times \int \frac{d^3 k''}{(2\pi)^3 2\omega_{k''}} \frac{f_N^2(p - k'')}{(m - \not{p} + \not{k}'')} \tilde{\Gamma}_N(k'', p). \end{aligned} \quad (4.53)$$

### 6. Inelasticity

As discussed in Sec. IIIC, the inelasticity of the  $N^*$  and the  $D_{13}$  is described by a fictitious  $\sigma^* N$  channel, where the  $\sigma^*$  is a scalar meson with the mass of two pions, and the couplings of the  $N^*$  and the  $D_{13}$  to this channel are given in Sec. IIIC. For simplicity, we assume that the photon does not couple *directly* to the inelastic channel, but it can couple *indirectly* through the process  $\gamma + N \rightarrow \{N^*, D_{13}\} \rightarrow \sigma^* + N$ , which takes place *without going through an intermediate  $\pi N$  channel*. These processes, which are not generated by the final state  $\pi N$  interactions, have been included in our model by adding them to the direct resonance pole driving terms in Fig. 1(a).

To accomplish this, the bare resonance propagators for the  $N^*$  and  $D_{13}$  are replaced by the inelastically dressed propagators

$$\begin{aligned} G_{N^*}(P) &= \frac{-i}{m_{N^*} - P + \Sigma_{N^*}^{inel}} \\ G_D^{i\mu\nu}(P) &= \frac{-i\Theta^{i\mu\nu}(P)}{m_D - P + \Sigma_D^{inel}}, \end{aligned} \quad (4.54)$$

where  $\Sigma_{N^*}^{inel}$  and  $\Sigma_D^{inel}$  the self energies of Roper and  $D_{13}$  *due to inelastic contributions only*. This replacement insures that *all* of the inelastic processes excited by the photon without passing through an intermediate  $\pi N$  state are included in the calculation. The inelastic self energies are

$$\begin{aligned} \Theta_{\alpha\beta}(P) \Sigma_D^{inel} &= \left(\frac{g'_{1D}}{\mu}\right)^2 f_D^2(P^2) \int \frac{d^3 k}{(2\pi)^3 2e_k} \Theta_{\alpha\lambda}(P) \frac{k^\lambda k^\rho f_N^2((P-k)^2)}{m - P + \not{k} - i\epsilon} \Theta_{\rho\beta}(P) \\ \Sigma_{N^*}^{inel} &= -(g'_{1N^*})^2 f_{N^*}^2(P^2) \int \frac{d^3 k}{(2\pi)^3 2e_k} \frac{f_N^2((P-k)^2)}{m - P + \not{k} - i\epsilon}, \end{aligned} \quad (4.55)$$

where the intermediate four momentum  $k = (e_k, \mathbf{k})$ , and  $e_k = \sqrt{m_{\sigma^*}^2 + k^2}$ .

### ACKNOWLEDGMENTS

It is a pleasure to acknowledge helpful conversations with Simon Capstick. This work was supported in part by the DOE under Grant No. DE-FG05-88ER40435.

## APPENDIX A: NOTATION AND ISOSPIN DECOMPOSITION

In this paper we adopt conventions designed to allow us to work as frequently as possible with terms which do not include a factor of  $i$  or the electric charge  $e$ . Starting with the Feynman rules (as found, for example, in Ref. [40]) we introduce the following conventions:

- All one body currents (i.e. three point currents) and propagators will be *multiplied by  $i$* .
- All hadronic vertex functions are left unchanged (i.e. *no* multiplication by  $i$ ).
- All four and five point currents, which would normally contain an overall factor of  $i$  (the Rule 0 of Ref. [40]) will be multiplied by an *additional* factor of  $i$ . If Rule 0 is omitted, this is equivalent to multiplying them by  $-1$ .
- The electric charge  $e > 0$  will be removed from all currents.

Using these rules, all four and five point currents are defined as in Eq. (2.15), and the basic nucleon Born term is real. Three point currents are all real, except for the  $\gamma + N \rightarrow \Delta$  transition current, Eq. (4.8), which now contains an extra factor of  $i$ .

The scattering  $S$  matrix for pion photoproduction is written in the following form:

$$S_{\pi\gamma}^{fi} = 1 - i(2\pi)^4 \delta^4(k' + p' - q - p) \frac{m}{\sqrt{4q\omega_k E_p E_{p'}}} M_{\pi\gamma}^{fi} \quad (\text{A1})$$

where  $k' = (\omega_k, \mathbf{k})$ ,  $q = (q, \mathbf{q})$ ,  $p = (E_p, \mathbf{p})$ ,  $p' = (E_{p'}, \mathbf{p}')$  are the four-momenta of the pion, photon, incoming and outgoing nucleon, respectively, and the energies are  $\omega_k = \sqrt{\mu^2 + \mathbf{k}^2}$ ,  $E_p = \sqrt{m^2 + \mathbf{p}^2}$ ,  $E_{p'} = \sqrt{m^2 + \mathbf{p}'^2}$ , with  $\mu$  and  $m$  the masses of the pion and nucleon.

Using the fact that the photon transforms as the sum of an isoscalar and the third component of an isovector, the isospin structure of the  $M_{\pi\gamma}$  matrix can be written:

$$M_{\pi\gamma} = M_{\pi\gamma}^+ \delta_{i3} + M_{\pi\gamma}^- \frac{1}{2} [\tau_i, \tau_3] + M_{\pi\gamma}^0 \tau_i, \quad (\text{A2})$$

where  $\tau_i$  and  $\tau_3$  are the Pauli spin matrices and  $i$  is the isospin index of the pion. The isovector transition amplitudes  $M_{\pi\gamma}^{(+,-)}$  may be expressed in terms of the amplitudes  $M_{\pi\gamma}^{(1/2,3/2)}$  with isospin 1/2 and 3/2 in the final state:

$$M_{\pi\gamma}^{1/2} = M_{\pi\gamma}^+ + 2M_{\pi\gamma}^- \quad M_{\pi\gamma}^{3/2} = M_{\pi\gamma}^+ - M_{\pi\gamma}^- \quad (\text{A3})$$

The isoscalar amplitude  $M_0$  always leads to a final state with isospin 1/2. The amplitudes for photoproduction from a proton are:

$$\begin{aligned} \left( M_{\pi\gamma}^{1/2} \right)_{\text{proton}} &= \frac{1}{3} (M_{\pi\gamma}^+ + 2M_{\pi\gamma}^- + 3M_{\pi\gamma}^0) \\ \left( M_{\pi\gamma}^{3/2} \right)_{\text{proton}} &= M_{\pi\gamma}^+ - M_{\pi\gamma}^- \end{aligned} \quad (\text{A4})$$

Each of these isospin scattering matrices may be expressed in terms of the operators  $O_{\pm}^i$

$$M = \sum_{i=1,2} O_{\pm}^i M_{i\pm} + O_{\pm}^i M_{i-}, \quad (\text{A5})$$

where

$$\begin{aligned} O_{\pm}^1 &= \frac{1}{2} (1 \pm \gamma^0) \not{\epsilon} \gamma_5 \\ O_{\pm}^2 &= \frac{1}{2} (1 \pm \gamma^0) 2\mathbf{k} \cdot \boldsymbol{\epsilon} \gamma_5 \end{aligned} \quad (\text{A6})$$

where, for an incoming photon traveling in the  $+\hat{z}$  direction, the photon polarization vector,  $\boldsymbol{\epsilon}$ , is

$$\boldsymbol{\epsilon}_{\lambda\gamma} = \frac{1}{\sqrt{2}} (-\lambda_{\gamma} \hat{\mathbf{x}} - i\hat{\mathbf{y}}), \quad (\text{A7})$$

where  $\lambda_{\gamma} = \pm 1$  is the photon helicity.

## APPENDIX B: MULTIPOLE AMPLITUDES

Denote the incoming and outgoing nucleon helicities by  $\lambda_N$  and  $\lambda_{N'}$ , respectively, and specialize the scattering to the  $xz$  plane (so that  $\phi = 0$ ). Following Jacob and Wick [43], the angular momentum decomposition of the helicity amplitudes  $M_{\lambda'\lambda}(\theta)$  is given by:

$$M_{\lambda'\lambda}(\theta) = \frac{1}{4\pi} \sum_j (2j+1) M_{\lambda'\lambda}^j d_{\lambda,\lambda'}^j(\theta) \quad (\text{B1})$$

where  $\lambda = \lambda_{\gamma} - \lambda_N$  and  $\lambda' = -\lambda_{N'}$ . Using the orthogonality of the  $d$  functions, the partial wave amplitudes are

$$M_{\lambda'\lambda}^j = 2\pi \int d\cos\theta M_{\lambda'\lambda}(\theta) d_{\lambda,\lambda'}^j(\theta). \quad (\text{B2})$$

The functions  $d_{\lambda\lambda'}^j$ , for  $j = 1/2$  and  $3/2$  are written explicitly in Appendix C. The orthogonality of these functions makes it easy to express the integrated cross section  $\sigma_{total}$  in terms  $M_{\lambda'\lambda}^j$ .

Now, since  $\lambda_\gamma = \pm 1$  for real, transverse photons, we have eight helicity amplitudes; however parity relates all the amplitudes with  $\lambda_\gamma = 1$  to those with  $\lambda_\gamma = -1$  (and opposite signs for  $\lambda_N$  and  $\lambda_{N'}$ ). Hence we need consider only those four amplitudes with  $\lambda_\gamma = 1$ . Remembering that  $\phi = 0$ , we can evaluate all of the operators  $\langle \lambda_{N'} | O_\pm^i | \lambda_N \rangle = \bar{u}(p', \lambda_{N'}) O_\pm^i u(p, \lambda_N)$ . In the center of mass system, where  $\mathbf{p} = -\mathbf{q}$  and  $\mathbf{p}' = -\mathbf{k}$  explicitly:

Helicity ++ :

$$\begin{aligned} \langle +|O_+^1|+ \rangle &= 0 \\ \langle +|O_-^1|+ \rangle &= 0 \\ \langle +|O_+^2|+ \rangle &= -\frac{1}{\sqrt{2}} \frac{z_2}{mz_1} |\mathbf{q}||\mathbf{k}| \sin \theta \cos \frac{1}{2}\theta \\ \langle +|O_-^2|+ \rangle &= \frac{1}{\sqrt{2}} \frac{z_1}{mz_2} |\mathbf{k}|^2 \sin \theta \cos \frac{1}{2}\theta \end{aligned} \quad (B3)$$

Helicity +-:

$$\begin{aligned} \langle +|O_+^1|- \rangle &= \frac{1}{\sqrt{2}} \frac{z_1 z_2}{m} \cos \frac{1}{2}\theta \\ \langle +|O_-^1|- \rangle &= -\frac{1}{\sqrt{2}} \frac{|\mathbf{q}||\mathbf{k}|}{mz_1 z_2} \cos \frac{1}{2}\theta \\ \langle +|O_+^2|- \rangle &= \frac{1}{\sqrt{2}} \frac{z_2 |\mathbf{q}||\mathbf{k}|}{mz_1} \sin \theta \sin \frac{1}{2}\theta \\ \langle +|O_-^2|- \rangle &= \frac{1}{\sqrt{2}} \frac{z_1 |\mathbf{k}|^2}{mz_2} \sin \theta \sin \frac{1}{2}\theta \end{aligned} \quad (B4)$$

Helicity -+:

$$\begin{aligned} \langle -|O_+^1|+ \rangle &= 0 \\ \langle -|O_-^1|+ \rangle &= 0 \\ \langle -|O_+^2|+ \rangle &= \frac{1}{\sqrt{2}} \frac{z_2 |\mathbf{q}||\mathbf{k}|}{mz_1} \sin \theta \sin \frac{1}{2}\theta \\ \langle -|O_-^2|+ \rangle &= \frac{1}{\sqrt{2}} \frac{z_1 |\mathbf{k}|^2}{mz_2} \sin \theta \sin \frac{1}{2}\theta \end{aligned} \quad (B5)$$

Helicity --:

$$\begin{aligned} \langle -|O_+^1|- \rangle &= -\frac{1}{\sqrt{2}} \frac{z_1 z_2}{m} \sin \frac{1}{2}\theta \\ \langle -|O_-^1|- \rangle &= -\frac{1}{\sqrt{2}} \frac{|\mathbf{q}||\mathbf{k}|}{mz_1 z_2} \sin \frac{1}{2}\theta \\ \langle -|O_+^2|- \rangle &= \frac{1}{\sqrt{2}} \frac{z_2 |\mathbf{q}||\mathbf{k}|}{mz_1} \sin \theta \cos \frac{1}{2}\theta \\ \langle -|O_-^2|- \rangle &= -\frac{1}{\sqrt{2}} \frac{z_1 |\mathbf{k}|^2}{mz_2} \sin \theta \cos \frac{1}{2}\theta \end{aligned} \quad (B6)$$

where  $z_1 = \sqrt{E_p + m}$  and  $z_2 = \sqrt{E_{p'} + m}$ .

Parity conserving amplitudes may be constructed from the helicity amplitudes by taking the following linear combinations:

$$\begin{aligned} A_{\ell+} &= -\frac{1}{\sqrt{2}} \frac{1}{4\pi} (M_{\frac{1}{2} \frac{1}{2}}^j + M_{-\frac{1}{2} \frac{1}{2}}^j) \\ A_{(\ell+1)-} &= \frac{1}{\sqrt{2}} \frac{1}{4\pi} (M_{\frac{1}{2} \frac{1}{2}}^j - M_{-\frac{1}{2} \frac{1}{2}}^j) \\ B_{\ell+} &= \frac{1}{\sqrt{2\ell(\ell+2)}} \frac{1}{4\pi} (M_{\frac{1}{2} \frac{3}{2}}^j + M_{-\frac{1}{2} \frac{3}{2}}^j) \quad \ell > 0 \\ B_{(\ell+1)-} &= -\frac{1}{\sqrt{2\ell(\ell+2)}} \frac{1}{4\pi} (M_{\frac{1}{2} \frac{3}{2}}^j - M_{-\frac{1}{2} \frac{3}{2}}^j) \quad \ell > 0 \end{aligned} \quad (B7)$$

where  $\ell = j - 1/2$ . The multipole amplitudes are obtained from the parity amplitudes using the following relations:

$$\begin{aligned} E_{\ell+} &= \frac{1}{\ell+1} (A_{\ell+} + \ell B_{\ell+}) \\ M_{\ell+} &= \frac{1}{\ell+1} (A_{\ell+} - (\ell+2) B_{\ell+}) \\ E_{(\ell+1)-} &= -\frac{1}{\ell+1} (A_{(\ell+1)-} - (\ell+2) B_{(\ell+1)-}) \\ M_{(\ell+1)-} &= \frac{1}{\ell+1} (A_{(\ell+1)-} + \ell B_{(\ell+1)-}) \end{aligned} \quad (B8)$$



## APPENDIX C: THE ROTATION MATRICES

$$j = \frac{1}{2}$$

$$\begin{aligned} d_{\frac{1}{2}\frac{1}{2}}^{1/2} &= d_{-\frac{1}{2}-\frac{1}{2}}^{1/2} = \cos \frac{1}{2}\theta \\ d_{\frac{1}{2}-\frac{1}{2}}^{1/2} &= -d_{-\frac{1}{2}\frac{1}{2}}^{1/2} = -\sin \frac{1}{2}\theta \end{aligned}$$

(C1)

$$j = \frac{3}{2}$$

$$\begin{aligned} d_{\frac{3}{2}\frac{1}{2}}^{3/2} &= -\sqrt{3} \cos^2 \frac{1}{2}\theta \sin \frac{1}{2}\theta \\ d_{\frac{1}{2}\frac{1}{2}}^{3/2} &= \cos \frac{1}{2}\theta (1 - 3 \sin^2 \frac{1}{2}\theta) \\ d_{\frac{3}{2}-\frac{1}{2}}^{3/2} &= \sqrt{3} \cos \frac{1}{2}\theta \sin^2 \frac{1}{2}\theta \\ d_{\frac{1}{2}-\frac{1}{2}}^{3/2} &= \sin \frac{1}{2}\theta (1 - 3 \cos^2 \frac{1}{2}\theta) \end{aligned}$$

(C2)

## REFERENCES

- [1] G.F. Chew, M.L. Goldberger, F.E. Low and Y. Nambu *Phys. Rev.* **106**, 1345(1957).
- [2] A. Donnachie, in High Energy Physics, ed. E. Burhop, vol 5, (Academic Press, New York, 1972) p. 1
- [3] M. G. Olsson and E.T Osypowski *Nucl. Phys.* **B87**,399 (1975) , *Phys. RevD***17** 174(1978), and M.G. Olsson *Nuc. Phys.* **B 78**, 55 (1974).
- [4] R.S. Wittman, R.M. Davidson and N.C. Mukhopadhyay *Phys. Lett.* **B142**, 336 (1984) ,R.M. Davidson N.C. Mukhopadhyay and R.S. Wittman *Phys. Rev.* **D43**, 71 (1991).
- [5] S. Nozawa, B. Blankleider, and T. S. H. Lee, *Nucl. Phys.* **A513**, 459 (1990).
- [6] T. S. H. Lee and B.C. Pearce *Nucl. Phys.* **A530**, 532 (1991).
- [7] Franz Gross and Yohanes Surya *Phys. Rev.* **C47**, 703 (1993).
- [8] R.A. Arndt, R.L. Workman, Zhujun Li and L. D. Roper *Phys. Rev. C* **42**, 1853 (1990).
- [9] K. M. Watson *Phys. Rev.* **95**, 228 (1954).
- [10] A.M. Bernstein, S. Nozawa, M.A. Moinester *Proc. of the Workshop on Hadron Structure from Photo-reaction at Intermediate Energies, BNL 1992* p. 68
- [11] Review of particle properties *Phys. Rev. D* **45**, 1 (1992).
- [12] H. Tanabe and K.Ohta *Phys. Rev. C* **31**, 1876 (1986).
- [13] S. N. Yang *J. Phys.* **G11**, L205 (1985).
- [14] R. Cenni, G. Dillon, and P.Christillin *Nuovo Cimento* **97A**, 1 (1987)
- [15] N.M. Kroll and M.A. Ruderman *Phys. Rev.* **93**, 233 (1954).
- [16] S. Fubini, G. Furlan and C. Rossetti *Nuovo Cimento* **40**, 1171 (1965).
- [17] E. Mazzucato et. al. *Phys. Rev. Lett* **57** 3144(1986)
- [18] R. Beck et al. *Phys. Rev. Lett.* **65**, 1841 (1990).
- [19] A.N. Kamal *Phys. Rev. Lett* **63**, 2346 (1989)
- [20] V. Bernard, N.Kaiser, J. Gasser, U. Meissner. *Phys. Lett.* **B18**, 291 (1991).
- [21] L.M. Nath and S.K. Singh *Phys. Rev. C* **39**, 1207 (1989).
- [22] T. Schafer and W.Weise *Phys. Lett.* **B 250**, 6 (1990).
- [23] H. W. L. Naus *Phys. Rev. C* **43**, R365 (1991).
- [24] A.M. Bernstein and B.R. Holstein *Comment on Nuclear and Particle Physics* Vol 20. No. 4, 197 (1991).
- [25] D. Drechsel and L. Tiator *J. Phys.* **G 18**, 449 (1992).
- [26] S. Fubini, Y. Nambu and V. Wataghin *Phys. Rev.* **111**, 329 (1958).
- [27] I. Blomqvist and J.M. Laget *Nucl. Phys. A* **280** 405(1977)
- [28] P. Noelle *Prog. Theor. Phys.* **60**, 778 (1978).
- [29] R.M. Davidson and N.C. Mukhopadhyay *Phys. Rev.* **D42**, 20(1990).

- [30] M. Araki and I. R. Afnan *Phys. Rev. C* **36**, 250 (1987).  
 [31] T.-S.H. Lee and B.C. Pearce *Nucl. Phys. A* **530**, 532 (1991).  
 [32] K. Ohta, *Phys. Rev. C* **40**, 1335 (1989); *ibid* **41**, 1213 (1990).  
 [33] H. W. L. Naus, J. H. Koch, and J. L. Friar *Phys. Rev. C* **41**, 2852 (1990).  
 [34] C.H.M. van Antwerpen and I.R. Afnan *Nucl-th Bull. Board 9308014* (August, 1993).  
 [35] F. L. Gross and D. O. Riska, *Phys. Rev. C* **36**, 1928 (1987).  
 [36] F. L. Gross, J. W. Van Orden and K. Holinde *Phys. Rev. C* **45**, 2094 (1992).  
 [37] E. Bovet *Phys. Lett.* **153B**, 231 (1985).  
 [38] R. Arndt and S. Roper, Scattering Analysis and Interactive Dial-in (SAID) program, Virginia Polytechnic Institute and State University.  
 [39] M. Benmerrouche, R. M. Davidson and N. C. Mukhopadhyay *Phys. Rev. C* **39**, 2339 (1989).  
 [40] F. Gross, *Relativistic Quantum Mechanics and Field Theory*, Wiley Interscience, 1993.  
 [41] H.F. Jones and M.D. Scadron *Ann. of Phys.* **81**, 1( 1973).  
 [42] H. Ito, W. W. Buck, and F. Gross *Phys. Rev. C* **43**, 2483 (1991); H. Ito and F. Gross *Phys. Rev. C* **48**, 1948 (1993).  
 [43] M. Jacob and G. C. Wick, *Ann. Phys.* **7**, 404 (1959).

TABLE I. The parameters of the  $\pi N$  model. Those in bold face were varied during the fit; the others are either fixed or determined by the fit.

<i>parameter</i>	<i>bare</i>	<i>dressed</i>
$g^2/4\pi$	13.5	13.3
$\lambda$	<b>0.200</b>	
$C$	0.884	
$C_\rho$	<b>0.674</b>	
$m^*$	<b>1431.8</b>	1442.2
$g_{N^*}^2/4\pi$	<b>3.590</b>	5.795
$\Gamma^*$		228.6
$Z(m)$		-0.0042
$Z(m^*)$		-0.0043 -0.023 <i>i</i>
$g_{1N^*}^{\prime 2}/4\pi$	<b>0.062</b>	
$g_{2N^*}^{\prime 2}/4\pi$	0.0	
$\Lambda$	<b>1225.4</b>	
$\Lambda^*$	<b>1853.7</b>	
$m_\Delta$	<b>1301.8</b>	1229.9
$g_\Delta^2/4\pi$	<b>0.813</b>	0.808
$\Gamma_\Delta$		123.9
$\Lambda_\Delta$	<b>1515.5</b>	
$m_D$	<b>1520.4</b>	1517.9
$g_D^2/4\pi$	<b>0.704</b>	0.698
$\Gamma_D$		124.5
$g_{1D}^{\prime 2}/4\pi$	<b>0.031</b>	
$g_{2D}^{\prime 2}/4\pi$	0.0	
$\Lambda_D$	<b>1829.3</b>	

TABLE II. The new parameters in the  $\gamma N$  the model. Those in bold face were varied during the fit; the others were fixed.

<i>parameter</i>	<i>value</i>
$g_{1N^*}$	<b>-0.231</b>
$g_{2N^*}$	<b>0.831</b>
$g_{1\Delta}$	<b>1.121</b>
$g_{2\Delta}$	<b>1.333</b>
$g_{1D}$	<b>-2.340</b>
$g_{2D}$	<b>-2.450</b>
$g_{\rho\pi\gamma}g_{\rho NN}$	<b>-0.439</b>
$g_{\omega\pi\gamma}g_{\omega NN}$	<b>8.168</b>
$f_{\rho NN}/g_{\rho NN}$	7.52525
$f_{\omega NN}/g_{\omega NN}$	<b>0.76</b>